



TECHNICKÁ UNIVERZITA V LIBERCI
Fakulta mechatroniky, informatiky
a mezioborových studií ■

Numerické modelování hydromechaniky v porézním prostředí

Diplomová práce

Studijní program: N3901 – Aplikované vědy v inženýrství
Studijní obor: 3901T055 – Aplikované vědy v inženýrství

Autor práce: **Bc. Svetlana Šaušová**
Vedoucí práce: Mgr. Jan Stebel, Ph.D.





TECHNICAL UNIVERSITY OF LIBEREC
Faculty of Mechatronics, Informatics
and Interdisciplinary Studies ■

Numerical modeling of hydromechanics in porous medium

Master thesis

Study programme: N3901 – Applied Science in Technology
Study branch: 3901T055 – Applied Science in Technology

Author: **Bc. Svetlana Šaušová**
Supervisor: Mgr. Jan Stebel, Ph.D.



ZADÁNÍ DIPLOMOVÉ PRÁCE

(PROJEKTU, UMĚLECKÉHO DÍLA, UMĚLECKÉHO VÝKONU)

Jméno a příjmení: **Bc. Svetlana Šaušová**
Osobní číslo: **M16000154**
Studijní program: **N3901 Aplikované vědy v inženýrství**
Studijní obor: **Aplikované vědy v inženýrství**
Název tématu: **Numerické modelování hydromechaniky v porézním prostředí**
Zadávající katedra: **Ústav nových technologií a aplikované informatiky**

Z á s a d y p r o v y p r a c o v á n í :

1. Seznamte se s problematikou matematického modelování a numerických metod pro proudění a deformace v hornině se zaměřením na využívání geotermální energie.
2. Formulujte model hydromechaniky pro rozpukanou horninu založený na Biotově poroelasticitě. Popište postup dimenzionální redukce a přechodové podmínky mezi horninou a puklinou.
3. Zvolte vhodnou diskretizaci 2D modelu, která bude stabilní pro malý časový krok a schopná popsat šíření puklin v předem známém směru.
4. Implementujte diskrétní problém ve vhodném softwarovém prostředí a proveďte výpočty:
 - modelové úlohy s referenčním nebo analytickým řešením,
 - kvazireálné úlohy hydraulické stimulace.Na základě provedených výpočtů zhodnoňte výhody a nevýhody numerické metody.
5. Text diplomové práce zpracujte v anglickém jazyce.



Rozsah grafických prací: **dle potřeby**
Rozsah pracovní zprávy: **40 - 60 stran**
Forma zpracování diplomové práce: **tištěná/elektronická**
Seznam odborné literatury:

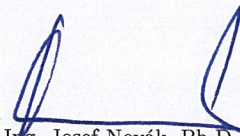
- [1] A. H.-D. Cheng: Poroelasticity. Springer, 2016.
- [2] V. Martin, J. Jaffré, J. E. Roberts: Modeling fractures and barriers as interfaces for flow in porous media, SIAM J. Sci. Comput. 26(5), 1667-1691, 2005.
- [3] T.-P. Fries, T. Belytschko: The extended/generalized finite element method: An overview of the method and its applications, Internat. J. Numer. Methods Engrg., 84, 253-304, 2010.

Vedoucí diplomové práce: **Mgr. Jan Stebel, Ph.D.**
Ústav nových technologií a aplikované informatiky

Datum zadání diplomové práce: **19. října 2017**
Termín odevzdání diplomové práce: **14. května 2018**


prof. Ing. Zdeněk Plíva, Ph.D.
děkan




Ing. Josef Novák, Ph.D.
vedoucí ústavu

V Liberci dne 19. října 2017

Prohlášení

Byla jsem seznámena s tím, že na mou diplomovou práci se plně vztahuje zákon č. 121/2000 Sb., o právu autorském, zejména § 60 – školní dílo.

Beru na vědomí, že Technická univerzita v Liberci (TUL) nezasahuje do mých autorských práv užitím mé diplomové práce pro vnitřní potřebu TUL.

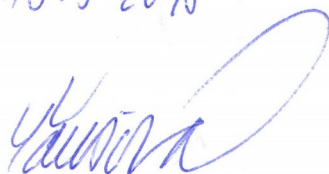
Užiji-li diplomovou práci nebo poskytnu-li licenci k jejímu využití, jsem si vědoma povinnosti informovat o této skutečnosti TUL; v tomto případě má TUL právo ode mne požadovat úhradu nákladů, které vynaložila na vytvoření díla, až do jejich skutečné výše.

Diplomovou práci jsem vypracovala samostatně s použitím uvedené literatury a na základě konzultací s vedoucím mé diplomové práce a konzultantem.

Současně čestně prohlašuji, že tištěná verze práce se shoduje s elektronickou verzí, vloženou do IS STAG.

Datum: 13. 5. 2018

Podpis:



Poděkování

V první řadě bych ráda poděkovala vedoucímu práce Mgr. Janu Stebelovi, Ph.D. za velkou trpělivost, cenné rady a za to obrovské množství času, jenž mi ochotně věnoval při tvorbě této práce. Děkuji svému příteli za jeho podporu, bez které bych tuto práci určitě nenapsala.

Abstrakt

Tato práce si stanovila dva cíle. Prvním je odvození modifikované verze Biotova systému parciálních diferenciálních rovnic pro oblast s redukovanou puklinou. Dalším z cílů je aproximace a numerické řešení tohoto modelu. Model je implementovaný pomocí softwarové knihovny FEniCS. Aplikací implementovaného modelu na konkrétní problém jsou vytvořeny dvě numerické simulace. Na základě výsledků, které poskytly tyto simulace, je posouzena funkčnost odvozeného modelu.

Klíčová slova: poroelasticita, hydraulické štěpení, diskretní puklina, FEniCS, numerické řešení, simulace

Abstract

This work has two main objectives. The first one is connected to modified version of Biot's system of partial differential equations for reduced fracture domain. The other one is approximation and numerical solution of this model. The model is implemented through the FEniCS software library. Two numerical simulations are made by application of the implemented model to a specific problem. The model functionality has been evaluated on the base of results obtained by the simulations.

Key words: poroelasticity, hydraulic fracturing, discrete fracture, FEniCS, numerical solution, simulation

Contents

Poděkování	v
Abstrakt	vi
Abstract	vii
List of Figures	ix
List of Symbols	x
1 Introduction	1
1.1 Hydraulic fracturing	2
1.2 Biot poroelasticity	4
1.3 Bibliography review	5
2 Biot model	8
2.1 Reduced model	8
2.2 Weak form	18
3 Numerical solution	25
3.1 Time and space discretization	25
3.1.1 Space discretization	25
3.1.2 Time discretization	27
3.2 FEniCS	29
3.3 Simulations	33
Summary	41
Bibliography	43
Appendix	44

List of Figures

1.1	<i>Hot Dry Rock scheme.</i>	3
2.1	<i>The domain Ω.</i>	9
3.1	<i>Conforming meshing, (Left): Two-dimensional domain Ω with a simplex mesh. (Right):The one-dimensional reduced fracture γ is meshed with the line segments.</i>	26
3.2	<i>The components of FEniCS.</i>	30
3.3	<i>Geometry of computational domain.</i>	33
3.4	<i>(Left):Boundary conditions (Dirichlet), (Right): Meshed domain for Simulation 1.</i>	34
3.5	<i>(Left):Boundary conditions (Dirichlet), (Right): Meshed domain for Simulation 2.</i>	35
3.6	<i>Pressure field progress in time $t = 50\Delta t, 200\Delta t$.</i>	37
3.7	<i>Pressure field progress in time $t = 300\Delta t, 500\Delta t$.</i>	38
3.8	<i>Displacement field progress in time $t = 50\Delta t, 200\Delta t$.</i>	39
3.9	<i>Displacement field progress in time $t = 300\Delta t, 500\Delta t$.</i>	40

List of Symbols

\mathbb{A} general tensor of anisotropy

\mathbb{C} elasticity tensor

d fracture width

f, F source

g gravitational constant

\mathbf{g}, \mathbf{G} source

\mathbb{I} identity tensor

\mathbb{K} hydraulic conductivity

N number of time steps

\mathbf{n} normal vector

p pressure

P average pressure in fracture

\mathbf{q} Darcy flux

S specific storage coefficient

\mathbf{u} displacement

U average displacement in fracture

α Biot coefficient

Γ domain boundary

γ reduced fracture domain

Δt time step

ε strain tensor

κ permeability

λ Lamé's first parameter

μ Lamé's second parameter (from Chapter 2.)

μ dynamic viscosity (in Chapter 1.)

ρ density

σ stress tensor

Ω domain

Chapter 1

Introduction

In present days, when the reserves of fossil fuels are decreasing and pollution of environment influences human health, the demands for alternative energy sources is rising. One of such source is the deep geothermal energy exploited in so-called *Hot Dry Rock* (HDR) systems. The construction as well as operation of HDR is a challenging task. In this work we focus on mathematical modelling of hydraulic fracturing, a process largely influencing the performance of HDR systems.

This work consists of three chapters. In the first one, we list a couple of industry applications where hydro-mechanical interaction in porous media (poroelasticity) takes place. We also describe the Biot system of poroelasticity which will be used in this work. We mention a few publications, which are related to for this work.

The second chapter is the essential part of this work, here we modify the original Biot equations for the case when the physical domain contains a thin fracture. In this chapter, we also derive variational formulation of our model.

The last chapter focuses on the numerical solution of our model. We use the Finite element method together with the implicit Euler timestepping for the approximation. Our model is implemented by help software library FEniCS. We compute numerical simulations for two cases. The geometry, initial and boundary conditions are common for both of simulations. A single difference between them is in meshing. At the end of the chapter we comment on the parameters which have important impact to quality of simulations.

1.1 Hydraulic fracturing

We would like to describe the creation and expansion of fractures during the process of hydraulic fracturing. It is very important to control composed fractures because of possible cracks into adjacent layers which can contain water. The hydraulic fracturing technique is being used e.g. in extraction of mineral oils. The oil can contaminate drinking water resources and mixture of oil and water is extremely hard to separate. It means that this technique can have potential harmful consequences on the environment. The method of hydraulic fracturing is not new. The first hydraulic fracturing experiment was performed in 1947 at the Hugoton gas field in Grant County of southwestern Kansas. Till 1970s, water-based fluids were not typically used as a fracturing fluid. Nowadays, the term *hydraulic fracturing* is usually connected only to the process of fracturing rock formation with water-based fluid.

A hydraulic fracture is formed by pumping the fracturing fluid under high pressure into a wellbore. If fluid pressure rate overcomes the rock strength then fluid helps to open or enlarge fracture in the geological formation. The fracture fluid has to contain *proppant*, which is an additional grainy material such as sand. Its function is to keep fracture from closing when pumping pressure releases. After that, the fracture fluid is drained back to the surface. Fractures of different width, length and direction can occur in geological formation but only certain types of fractures are suitable for particular industry applications. Design of hydraulic fracturing is a complex problem with many unknowns. It is possible to partly influence cracking into only one type or direction. This selection is made by changes of pressure or a kind of the fracture fluid.

In the past, the main application of hydraulic fracturing was *fracking*. It is an unconventional method of oil extraction. Nowadays, hydraulic fracturing is used not only in oil and gas industry, but also in a number of other applications, such as injection of liquid nuclear waste into deep geological formation for isolation and disposal, using water or CO_2 as injection fluid to create fracture to circulate water in enhanced geothermal system (*HDR*), creating horizontal fracture as a means of enhancing pump-and-treat, soil vapor extraction, and in situ environmental remediation in shallow soil, for pollutants such as heavy metals and hydrocarbon waste or spills and stimulating groundwater production by connecting naturally occurring fractures in rock formation [10].

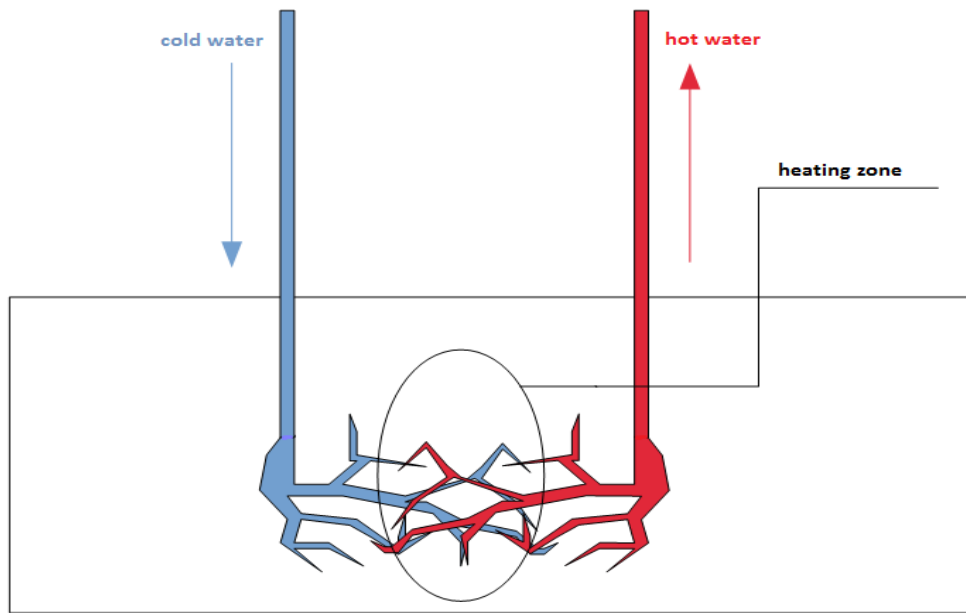


Figure 1.1: *Hot Dry Rock scheme.*

The hydraulic fracturing technique now takes a different aim - instead of creating a single, large fracture from a vertical well, it aims at the creation of a large number of shorter, closely spaced and interconnecting fractures from a horizontal well. The technique allows the production from the unconventional reservoir such as shale gas formation, also known as *tight gas reservoir*. "Tight" means very low permeability such that production using conventional technique is not economically feasible. The fracking technology opens the door for production of the vast reserve of shale gas and shale oil, thus extending the world's energy prospect. The practice of fracking, however is controversial as it creates many environmental concerns [10].

The main motivation for creation of this work is to improve the hydraulic fracturing process for better utilization of geothermal energy by HDR technique. In present days, hydrothermal technology *Hot Wet Rock (HWR)* is being widely used. HWR technique operates with a hot water found naturally in the bed-rock. Disadvantage of this technology is its geographically limited application. There are only a few places where the water is in the reachable depth and it is possible to use HWR.

In opposition, many dry places exist in terrestrial crust, which are reachable by drilling, and accumulate a huge amount of heat. These places can be used for HDR. The principle of HDR is pumping of a cool water under high pressure through a well into the deep fracture reservoir, where the cool water is heated above

boiling temperature (see Figure 1.1). After that the hot water is taken back to the surface throughout another well to flash to steam in an electricity generating plant. Commonly it is necessary to create a much more extensive fracture system like it is usually created naturally. Also, we have another demands for fracture reservoir, such as vastness. It is very important to create **connected** network of fractures. These artificial fractures are made by *hydraulic fracturing technique*.

1.2 Biot poroelasticity

Our model of hydro-mechanical interactions will be based on *Biot's theory of poroelasticity*. In 1941, Belgian-American applied physicist Maurice Anthony Biot introduced a first general 3-dimensional theory of elastic deformation in saturated solid medium [3]. It was a great progress from earlier *Terzaghi* theory [16] that operated with the assumption of incompressible constituents. But the new Biot's theory still had some restrictions, since it was derived only for the isotropic case. During 1950s, Biot extended his original theory to general anisotropic case [4] (1955) and also derived an equation for dynamic response of porous media [5] (1956). The linear theory introduced by Biot was modified in 1969 by *Verruijt*. He made the theory more suitable for using in solid mechanics problems [17]. Until the year 1973, all Biot's theories had been operating with assumption of linear elasticity. In that time, Biot again made his theory more complex and general. He integrated a possibility of non-linear elasticity [6].

We consider a medium that consists of solid skeleton hereafter called *matrix* and of *pore fluid*. Change of the whole domain depends on matrix deformation and fluid behaviour. We assume that the liquid phase is incompressible and the solid phase is compressible in our model. The theory is connecting two physical laws.

The first one is the semi-empiric *Darcy law* for fluid flow in porous medium:

$$\mathbf{q} = -\frac{\kappa}{\mu}\nabla p, \quad (1.1)$$

where κ is a permeability of medium, viscosity is defined by μ , p refers to total pressure drop (from atmospheric pressure). Vector \mathbf{q} is called Darcy flux or Darcy velocity and describes discharge per unit area. In later application there will be

permeability κ substituted by *hydraulic conductivity* defined as:

$$\mathbb{K} = \frac{\kappa \rho g}{\mu} \mathbb{A}$$

where \mathbb{A} is a general tensor of anisotropy, ρ is the density of the fluid and g is the gravitational constant. The second material law included in Biot's theory is *the Hook law of linear elasticity*:

$$\boldsymbol{\sigma} = \mathbb{C} \boldsymbol{\varepsilon}, \quad (1.2)$$

where $\boldsymbol{\sigma}$ is a second order *stress tensor*, $\boldsymbol{\varepsilon}$ refers to second order *strain tensor* and \mathbb{C} is a fourth order elasticity tensor also called stiffness tensor.

Biot's theory gets out of the presumption of an internal stress decomposition for saturated porous medium. The whole internal stress can be divided into two parts. One part causes deformation of matrix, this behaviour describes the equation of *balance of forces* in rock:

$$-\nabla \cdot \boldsymbol{\sigma} + \alpha \nabla p = \mathbf{g}, \quad (1.3)$$

where $-\nabla \cdot \boldsymbol{\sigma}$ represents internal pressure, which is well known as an *effective stress*. The *pore pressure* is involved in the expression $\alpha \nabla p$ and \mathbf{g} refers to a *volume force*. The second part causes the change of pore-pressure and it subsequently activates fluid flow. The fluid behaviour is defined by the law of *conservation of mass* in fluid:

$$\partial_t (Sp + \alpha \nabla \cdot \mathbf{u}) - \nabla \cdot \mathbf{q} = f, \quad (1.4)$$

where the first term is the temporal increment of the *fluid content*, the changes of *Darcy flux* are described by $\nabla \cdot \mathbf{q}$ and f is a volume source. The PDE system (1.3), (1.4) with the constitutive relations (1.1), (1.2) is called the *Biot system*.

1.3 Bibliography review

Many specialized publications have been dedicated to modeling of flow in a porous material with fractures in last decade. [13] is one of the most cited articles. Model domain introduced in that paper is composed of two subdomains which are separated by an interface. The authors use the fact that fractures have in general

negligible its width in comparison with their length. Computational domain is made of two bulk spaces with the difference in permeability and the fracture which is treated as interface between these bulk spaces. The authors show that it is possible to derive the Darcy equation separately for each of subdomains and sequentially couple them by appropriate boundary conditions. The boundary conditions for fracture interface are defined with the help of the normal part of vector unknowns from equations for bulk spaces. The vector unknowns are divided into normal and tangential part for this reason.

Elder simulation needed to redefine mesh for every change in computational domain e.g. when a fracture was spreading. In modern numerical modeling of crack growth processes, the *eXtended Finite Element Method (XFEM)* is often used, which enriches the discrete function spaces by the functions locally reproducing the discontinuity along the fracture and the stress singularities at the crack tip. XFEM overcomes the need to adapt the mesh to the discontinuities and singularities of the solution. In the article [11], the authors work with a model domain which consists of porous medium with single fracture subdomain. The fracture does not have to proceed through the whole domain, fracture start and tip can be within the domain. Equations for bulk and fracture domain are coupled by the equality of pressures on the boundary between them and by continuity of normal fluxes through this boundary. Presented numerical solution is a combination of XFEM for matrix (skeleton) changes and lower dimensional finite elements for fluid flow.

Ruijie Liu in his dissertation thesis [12] focused on the derivation of *Discontinuous Galerkin method* for poroelasticity problem and on the comparison of *Continuous Galerkin (CG)* and *Discontinuous Galerkin (DG)* finite element method for poromechanics, elastic and poroelastic problem. Majority of current available commercial programs solve these problems by *CG FEM*. But in solutions given by these programs nonphysical oscillations can occur in low permeability zones. CG also is not able to correctly simulate problems, where discontinuity jumps are in pressure or temperature field. Because CG always gives a smooth solution. Liu studied stability analysis of CG for poroelastic problem. The author tried to abolish this numerical problem with help of DG FEM. Local mass and momentum conservation are also added to DG. This properties can be key for elimination of the oscillations and correct simulation of the jumps in fields.

Our work is mainly motivated by these three publications. We use similar reduction of fracture like is present in [13] and [11]. But we extend the theory

presented in [13] also to elasticity. Our model is also distinguished from *Hanowski and Sander's* model, we do not use *XFEM* and we also use only *linear model*, but we solve the nonstationary problem.

Chapter 2

Biot model

2.1 Reduced model

For the modelling of hydro-mechanical interaction in porous media we will use the Biot system:

$$\partial_t(Sp + \alpha \nabla \cdot \mathbf{u}) - \nabla \cdot (\mathbb{K} \nabla p) = f \quad \text{in } (0, T) \times \Omega, \quad (2.1)$$

$$-\nabla \cdot (\mathbb{C} \varepsilon(\mathbf{u}) - \alpha p \mathbb{I}) = \mathbf{g} \quad \text{in } (0, T) \times \Omega. \quad (2.2)$$

Here Ω is a bounded domain in \mathbb{R}^n , $n = 2$ or 3 and $(0, T)$ is a finite time interval. Symbols \mathbf{u} , p are the unknown displacement and pressure, respectively, S is the specific storage coefficient (inverse of the Biot modulus M), α stands for the Biot coefficient, \mathbb{K} is the tensor of hydraulic conductivity, \mathbb{C} is the fourth-order elastic tensor, \mathbb{I} denotes the unit second-order tensor and f , \mathbf{g} is the source and body force, respectively. The symbol $\varepsilon(\mathbf{u})$ stands for the symmetric part of the displacement gradient:

$$\varepsilon_{kl}(\mathbf{u}) := \frac{1}{2} \left[\frac{\partial u_k}{\partial x_l} + \frac{\partial u_l}{\partial x_k} \right].$$

On the external boundary we shall assume for simplicity the homogeneous Dirichlet conditions:

$$\begin{aligned} p &= 0 & \text{on } (0, T) \times \partial\Omega, \\ \mathbf{u} &= \mathbf{0} & \text{on } (0, T) \times \partial\Omega. \end{aligned}$$

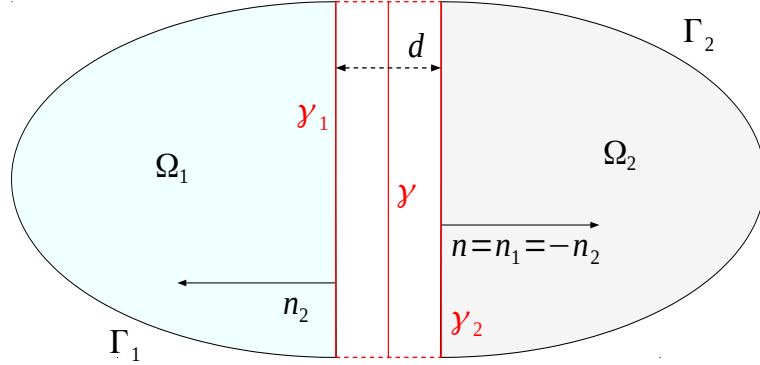


Figure 2.1: *The domain Ω .*

For completeness, we also need the initial condition for the pressure

$$p(0, \cdot) = p_0 \quad \text{in } \Omega.$$

Equations (2.1) and (2.2) describe the flow and linear elasticity in a saturated porous medium. In what follows, we will adapt (1)-(2) to a domain containing a fracture. We will therefore assume that the domain Ω , where Biot's model is considered, can be divided into 3 parts (see Figure 2.1):

$$\Omega = \Omega_1 \cup \Omega_2 \cup \Omega_f. \quad (2.3)$$

The symbol Ω_f denotes the fracture which separates two subdomains Ω_1 and Ω_2 . We shall further assume that the fracture can be written as follows:

$$\Omega_f = \left\{ \mathbf{x} + a\mathbf{n}; a \in (-d/2, d/2), \mathbf{x} \in \gamma \right\},$$

where γ is a $(n-1)$ -dimensional manifold representing the center of the fracture, \mathbf{n} is the unit normal vector to γ pointing from Ω_1 to Ω_2 and d denotes the cross-section of the fracture. We define the lateral boundaries γ_1, γ_2 of the domain Ω_f :

$$\gamma_i = \partial\Omega_i \cap \partial\Omega_f.$$

To distinguish between the functions defined in Ω_1 , Ω_2 , Ω_f , we shall use the notation $\mathbf{u}_i := \mathbf{u}|_{\Omega_i}$, $p_i := p|_{\Omega_i}$, $i = 1, 2, f$. The boundary conditions, which describe pressure and displacement on γ_i are the following ones:

$$\begin{aligned} p_i &= p_f, \quad (\mathbb{K}\nabla p_i \cdot \mathbf{n})|_{\Omega_i} = (\mathbb{K}\nabla p_f \cdot \mathbf{n})|_{\Omega_f}, \quad (0, T) \times \gamma_i, \quad i = 1, 2, \\ \mathbf{u}_i &= \mathbf{u}_f, \quad (\mathbb{C}\varepsilon(\mathbf{u}_i)\mathbf{n} - \alpha p_i \mathbf{n})|_{\Omega_i} = (\mathbb{C}\varepsilon(\mathbf{u}_f)\mathbf{n} - \alpha p_f \mathbf{n})|_{\Omega_f}, \quad (0, T) \times \gamma_i, \quad i = 1, 2, \end{aligned} \quad (2.4)$$

We will consider a few assumptions for our model parameters. The first of our assumptions is that hydraulic tensor \mathbb{K} , parameters α , S and the elastic tensor \mathbb{C} are constant in the bulk spaces Ω_1 , Ω_2 . All of these model parameters are also constant in the fracture domain Ω_f but its numeric value is different from the bulk domain. We will use notation $\mathbb{K}_f, S_f, \alpha_f, \mathbb{C}_f$ for restriction of parameters on fracture domain (for example $\mathbb{K}_f = \mathbb{K}|_{\Omega_f}$). The second assumption is that tensor \mathbb{K}_f is possible to divide into normal and tangential part $\mathbb{K}_f = k(\mathbf{n} \otimes \mathbf{n}) + \mathbb{K}_f(\mathbb{I} - \mathbf{n} \otimes \mathbf{n})$. Finally, we assume that the fracture is filled by an isotropic elastic medium i.e.:

$$\mathbb{C}_f \varepsilon(\mathbf{u}_f) = 2\mu_f \varepsilon(\mathbf{u}_f) + \lambda_f \text{tr}(\varepsilon(\mathbf{u}_f))\mathbb{I} = 2\mu_f \varepsilon(\mathbf{u}_f) + \lambda_f (\nabla \cdot \mathbf{u}_f)\mathbb{I}. \quad (2.5)$$

Following the approach of [Martin et al. (2005)], we will replace the thin domain Ω_f by γ and derive a modified system of equations for the averaged displacement and pressure in γ . In Ω_f , equation (2.1) reads:

$$\underbrace{\partial_t(S_f p_f + \alpha_f \nabla \cdot \mathbf{u}_f)}_A - \underbrace{\nabla \cdot (\mathbb{K}_f \nabla p_f)}_B = \underbrace{f}_C. \quad (2.6)$$

We start by integrating (2.6) across the fracture. For $\mathbf{x} \in \gamma$ we define $\int_{-\frac{d}{2}}^{\frac{d}{2}} a(\mathbf{x}) d\mathbf{n} := \int_{-\frac{d}{2}}^{\frac{d}{2}} a(\mathbf{x} + t\mathbf{n}) dt$. Let $\mathbf{v}_n := (\mathbf{v} \cdot \mathbf{n})\mathbf{n}$, $\mathbf{v}_\tau := \mathbf{v} - \mathbf{v}_n$ denote the normal and tangential part of a vector \mathbf{v} , respectively. For a tensor \mathbb{A} we define $\mathbb{A}_n := \mathbb{A}(\mathbf{n} \otimes \mathbf{n})$ and $\mathbb{A}_\tau := \mathbb{A} - \mathbb{A}_n$. Also, we define the tangential and normal

divergence and gradient as follows:

$$\begin{aligned}
\nabla^\tau \cdot \mathbf{v} &:= \nabla \cdot \mathbf{v}_\tau, \\
\nabla^n \cdot \mathbf{v} &:= \nabla \cdot \mathbf{v}_n, \\
\nabla^\tau q &:= (\nabla q)_\tau, \\
\nabla^n q &:= (\nabla q)_n, \\
\nabla^\tau \mathbf{v} &:= (\nabla \mathbf{v})_\tau, \\
\nabla^n \mathbf{v} &:= (\nabla \mathbf{v})_n, \\
\nabla^n \cdot \mathbb{A} &:= \nabla \cdot ((\mathbf{n} \otimes \mathbf{n})\mathbb{A}) = (\nabla(\mathbb{A}^T \mathbf{n}))\mathbf{n}, \\
\nabla^\tau \cdot \mathbb{A} &:= \nabla \cdot \mathbb{A} - \nabla^n \cdot \mathbb{A}.
\end{aligned}$$

Splitting the divergence $\nabla \cdot \mathbf{u}_f$ into the tangential and normal part,

$$\nabla \cdot \mathbf{u}_f = \nabla^\tau \cdot \mathbf{u}_f + \nabla^n \cdot \mathbf{u}_f, \quad (2.7)$$

and integrating \mathbb{A} across the fracture we obtain:

$$\begin{aligned}
\int_{-\frac{d}{2}}^{\frac{d}{2}} \mathbb{A} d\mathbf{n} &= \int_{-\frac{d}{2}}^{\frac{d}{2}} S_f p_f + \alpha_f (\nabla^\tau \cdot \mathbf{u}_f + \nabla^n \cdot \mathbf{u}_f) d\mathbf{n} \\
&= S_f \int_{-\frac{d}{2}}^{\frac{d}{2}} p_f d\mathbf{n} + \alpha_f \int_{-\frac{d}{2}}^{\frac{d}{2}} \nabla^\tau \cdot \mathbf{u}_f d\mathbf{n} + \alpha_f \int_{-\frac{d}{2}}^{\frac{d}{2}} \nabla^n \cdot \mathbf{u}_f d\mathbf{n}.
\end{aligned}$$

The integral $\int_{-\frac{d}{2}}^{\frac{d}{2}} \nabla^n \cdot \mathbf{u}_f d\mathbf{n}$ can be expressed as follows:

$$\int_{-\frac{d}{2}}^{\frac{d}{2}} \nabla^n \cdot \mathbf{u}_f = (\mathbf{u}_{f,n}|_{\gamma_2} - \mathbf{u}_{f,n}|_{\gamma_1}) \cdot \mathbf{n} = (\mathbf{u}_2|_{\gamma_2} - \mathbf{u}_1|_{\gamma_1}) \cdot \mathbf{n} \quad (2.8)$$

and hence we get:

$$\begin{aligned}
\int_{-\frac{d}{2}}^{\frac{d}{2}} \mathbb{A} d\mathbf{n} &= S_f \int_{-\frac{d}{2}}^{\frac{d}{2}} p_f d\mathbf{n} + \alpha_f \nabla^\tau \cdot \int_{-\frac{d}{2}}^{\frac{d}{2}} \mathbf{u}_{f,\tau} d\mathbf{n} + \alpha_f (\mathbf{u}_2|_{\gamma_2} - \mathbf{u}_1|_{\gamma_1}) \cdot \mathbf{n} \\
&= S_f dP + \alpha_f d\nabla^\tau \cdot \mathbf{U} + \alpha_f (\mathbf{u}_2|_{\gamma_2} - \mathbf{u}_1|_{\gamma_1}) \cdot \mathbf{n},
\end{aligned} \quad (2.9)$$

where

$$\mathbf{U} := \frac{1}{d} \int_{-\frac{d}{2}}^{\frac{d}{2}} \mathbf{u}_f d\mathbf{n} \quad \text{and} \quad P := \frac{1}{d} \int_{-\frac{d}{2}}^{\frac{d}{2}} p_f d\mathbf{n},$$

represent the average displacement and the average pressure in the fracture. Our next step is to integrate B:

$$\begin{aligned} \int_{-\frac{d}{2}}^{\frac{d}{2}} B d\mathbf{n} &= -\nabla \cdot \int_{-\frac{d}{2}}^{\frac{d}{2}} \mathbb{K}_f (\nabla^\tau p_f + \nabla^n p_f) d\mathbf{n} \\ &= -\nabla \cdot \left(\mathbb{K}_{f,\tau} \int_{-\frac{d}{2}}^{\frac{d}{2}} \nabla^\tau p_f d\mathbf{n} + \mathbb{K}_{f,n} (\mathbf{p}_{f,n}|_{\gamma_2} - \mathbf{p}_{f,n}|_{\gamma_1}) \right), \end{aligned}$$

where $\mathbf{p}_{f,n} := p_f \mathbf{n}$ is the normal part of pressure vector in the fracture. Using P , we can rewrite the last expression into the form

$$\int_{-\frac{d}{2}}^{\frac{d}{2}} B d\mathbf{n} = -\nabla \cdot \left(d \mathbb{K}_{f,\tau} \nabla^\tau P - \mathbb{K}_{f,n} (\mathbf{p}_{f,n}|_{\gamma_2} - \mathbf{p}_{f,n}|_{\gamma_1}) \right). \quad (2.10)$$

In (2.10), we will use an approximation of the pressure gradient on the borders of the fracture, which represents the flow between surrounding and the fracture through the borders. Expressions with pressure gradient will be approximated as follows:

$$\begin{aligned} \nabla^n \cdot (\mathbb{K}_{f,n} p_f|_{\gamma_2} \mathbf{n}) &\approx \underbrace{\mathbb{K}_f \mathbf{n} \cdot \mathbf{n}}_k \frac{p_2|_{\gamma_2} - P}{\frac{d}{2}}, \\ \nabla^n \cdot (\mathbb{K}_{f,n} p_f|_{\gamma_1} \mathbf{n}) &\approx \underbrace{\mathbb{K}_f \mathbf{n} \cdot \mathbf{n}}_k \frac{P - p_1|_{\gamma_1}}{\frac{d}{2}}. \end{aligned} \quad (2.11)$$

Consequently,

$$\int_{-\frac{d}{2}}^{\frac{d}{2}} B d\mathbf{n} = -k \left(\frac{p_2 - P}{\frac{d}{2}} - \frac{P - p_1}{\frac{d}{2}} \right) - \nabla \cdot d \mathbb{K}_{f,\tau} \nabla^\tau P. \quad (2.12)$$

The last part of equation (2.6) is on the right side. Introducing $F := \frac{1}{d} \int_{-\frac{d}{2}}^{\frac{d}{2}} f d\mathbf{n}$ we obtain:

$$\int_{-\frac{d}{2}}^{\frac{d}{2}} C d\mathbf{n} = \int_{-\frac{d}{2}}^{\frac{d}{2}} f d\mathbf{n} = d F. \quad (2.13)$$

After joining expressions (2.9), (2.12) and (2.13) we get the averaged Darcy equa-

tion in γ :

$$\begin{aligned} & \partial_t \left[S_f d P + \alpha_f d \nabla^\tau \cdot \mathbf{U} + \alpha_f (\mathbf{u}_2|_{\gamma_2} - \mathbf{u}_1|_{\gamma_1}) \cdot \mathbf{n} \right] - \dots \\ & \dots - k \left(\frac{p_2 - P}{\frac{d}{2}} - \frac{P - p_1}{\frac{d}{2}} \right) - \nabla^\tau \cdot \left(d \mathbb{K}_{f,\tau} \nabla^\tau P \right) = F d, \end{aligned} \quad (2.14)$$

which, after rearrangement, has the final form:

$$\begin{aligned} & d \left(\partial_t \left[S_f P + \alpha_f \nabla^\tau \cdot \mathbf{U} \right] - \nabla^\tau \cdot (\mathbb{K}_{f,\tau} \nabla^\tau P) \right) + \dots \\ & \dots + \alpha_f \partial_t (\mathbf{u}_2|_{\gamma_2} - \mathbf{u}_1|_{\gamma_1}) \cdot \mathbf{n} - \sum_{i=1}^2 \frac{2}{d} k (p_i|_{\gamma_i} - P) = F d. \end{aligned} \quad (2.15)$$

Now, move our attention on the second equation (2.2) from the Biot's model

$$-\nabla \cdot (\mathbb{C}_f \varepsilon(\mathbf{u}_f) - \alpha_f p_f \mathbb{I}) = \mathbf{g} \quad \text{in } (0, T) \times \Omega_f. \quad (2.16)$$

Here, multiplication of elasticity tensor \mathbb{C} and deformation tensor ε is defined by the expression (2.5). When we use (2.5) in the equation (2.16) then we get:

$$-\nabla \cdot (2\mu_f \varepsilon(\mathbf{u}_f)) - \nabla (\lambda_f \nabla \cdot \mathbf{u}_f) + \nabla (\alpha_f p_f) = \mathbf{g}. \quad (2.17)$$

Again, we divide the divergence and the gradient into the normal and tangential direction. We also start by integrating (2.17) across the fracture.

$$\int_{-\frac{d}{2}}^{\frac{d}{2}} -(\nabla^n \cdot + \nabla^\tau \cdot) (2\mu_f \varepsilon(\mathbf{u}_f)) d\mathbf{n} - \int_{-\frac{d}{2}}^{\frac{d}{2}} (\nabla^n + \nabla^\tau) (\lambda_f \text{tr}(\varepsilon(\mathbf{u}_f)) - \alpha_f p_f) d\mathbf{n} = \int_{-\frac{d}{2}}^{\frac{d}{2}} \mathbf{g} d\mathbf{n}. \quad (2.18)$$

For better orietation we will divide the equation into several terms which will be

treated separately.

$$\begin{aligned}
& - \underbrace{\int_{-\frac{d}{2}}^{\frac{d}{2}} \nabla^n \cdot (2\mu_f \varepsilon(\mathbf{u}_f)) d\mathbf{n}}_{A_1} - \underbrace{\int_{-\frac{d}{2}}^{\frac{d}{2}} \nabla^\tau \cdot (2\mu_f \varepsilon(\mathbf{u}_f)) d\mathbf{n}}_{A_2} - \underbrace{\int_{-\frac{d}{2}}^{\frac{d}{2}} \nabla^\tau (\lambda_f \operatorname{tr}(\varepsilon(\mathbf{u}_f)) - \alpha_f p_f) d\mathbf{n}}_{B_1} \\
& - \underbrace{\int_{-\frac{d}{2}}^{\frac{d}{2}} \nabla^n (\lambda_f \operatorname{tr}(\varepsilon(\mathbf{u}_f)) - \alpha_f p_f) d\mathbf{n}}_{B_2} = \int_{-\frac{d}{2}}^{\frac{d}{2}} \mathbf{g} d\mathbf{n}.
\end{aligned} \tag{2.19}$$

After using definition of deformation tensor ε_{kl} , the identity $\operatorname{tr}(\varepsilon(\mathbf{u}_f)) = \nabla \cdot \mathbf{u}_f$ and also assumption $\lambda_f = \text{constant}$, in the equation (2.19) we obtain:

$$\begin{aligned}
B_1 &= \int_{-\frac{d}{2}}^{\frac{d}{2}} \nabla^\tau \left(\lambda_f \nabla \cdot \mathbf{u}_f - \alpha_f p_f \right) d\mathbf{n} \\
&= \int_{-\frac{d}{2}}^{\frac{d}{2}} \nabla^\tau (\lambda_f \nabla \cdot \mathbf{u}_f) - \alpha_f \nabla^\tau p_f d\mathbf{n} \\
&= \lambda_f \int_{-\frac{d}{2}}^{\frac{d}{2}} \nabla^\tau (\nabla^\tau \cdot + \nabla^n \cdot) \mathbf{u}_f d\mathbf{n} - \alpha_f \nabla^\tau \left(\int_{-\frac{d}{2}}^{\frac{d}{2}} p_f d\mathbf{n} \right).
\end{aligned}$$

In this equation we again use (2.8) and replace integrals by P and \mathbf{U} :

$$\begin{aligned}
B_1 &= \lambda_f \int_{-\frac{d}{2}}^{\frac{d}{2}} \nabla^\tau (\nabla^\tau \cdot \mathbf{u}_f) d\mathbf{n} + \lambda_f \int_{-\frac{d}{2}}^{\frac{d}{2}} \nabla^\tau (\nabla^n \cdot \mathbf{u}_f) d\mathbf{n} - \alpha_f d\nabla^\tau P \\
&= \lambda_f d\nabla^\tau (\nabla^\tau \cdot \mathbf{U}) + \lambda_f \nabla^\tau ((\mathbf{u}_2|_{\gamma_2} - \mathbf{u}_1|_{\gamma_1}) \cdot \mathbf{n}) - \alpha_f d\nabla^\tau P.
\end{aligned} \tag{2.20}$$

We continue with part B_2 :

$$\begin{aligned}
B_2 &= \int_{-\frac{d}{2}}^{\frac{d}{2}} \nabla^n (\lambda_f \operatorname{tr}(\varepsilon(\mathbf{u}_f)) - \alpha_f p_f) d\mathbf{n} \\
&= \lambda_f \int_{-\frac{d}{2}}^{\frac{d}{2}} \nabla^n (\nabla \cdot \mathbf{u}_f) d\mathbf{n} + \alpha_f \int_{-\frac{d}{2}}^{\frac{d}{2}} \nabla^n p_f d\mathbf{n} \\
&= \lambda_f \int_{-\frac{d}{2}}^{\frac{d}{2}} \nabla^n (\nabla \cdot \mathbf{u}_f) d\mathbf{n} - \alpha_f (\mathbf{p}_2|_{\gamma_2} - \mathbf{p}_1|_{\gamma_1}) \\
&= \lambda_f (\nabla \cdot \mathbf{u}_f|_{\gamma_2} - \nabla \cdot \mathbf{u}_f|_{\gamma_1}) \mathbf{n} - \alpha_f (\mathbf{p}_2|_{\gamma_2} - \mathbf{p}_1|_{\gamma_1}) \\
&= \lambda_f (\nabla^n \cdot \mathbf{u}_f|_{\gamma_2} - \nabla^n \cdot \mathbf{u}_f|_{\gamma_1}) \mathbf{n} + \lambda_f (\nabla^\tau \cdot (\mathbf{u}_2|_{\gamma_2} - \mathbf{u}_1|_{\gamma_1})) \mathbf{n} - \alpha_f (\mathbf{p}_2|_{\gamma_2} - \mathbf{p}_1|_{\gamma_1}),
\end{aligned}$$

where we have to approximate parts with divergence of displacement in normal direction:

$$\begin{aligned}\nabla^n \cdot \mathbf{u}_f|_{\gamma_2} &\approx \frac{(\mathbf{u}_2|_{\gamma_2} - \mathbf{U}) \cdot \mathbf{n}}{\frac{d}{2}}, \\ \nabla^n \cdot \mathbf{u}_f|_{\gamma_1} &\approx \frac{(\mathbf{U} - \mathbf{u}_1|_{\gamma_1}) \cdot \mathbf{n}}{\frac{d}{2}}.\end{aligned}$$

After substitution of the approximations we obtain the final form of B_2 part:

$$\begin{aligned}B_2 &\approx \lambda_f \left(\frac{(\mathbf{u}_2|_{\gamma_2} - \mathbf{U}) \cdot \mathbf{n}}{\frac{d}{2}} - \frac{(\mathbf{U} - \mathbf{u}_1|_{\gamma_1}) \cdot \mathbf{n}}{\frac{d}{2}} \right) \mathbf{n} + \dots \\ &\dots + \lambda_f \left(\nabla^\tau \cdot (\mathbf{u}_2|_{\gamma_2} - \mathbf{u}_1|_{\gamma_1}) \right) \mathbf{n} - \alpha_f (p_2 \mathbf{n}|_{\gamma_2} - p_1 \mathbf{n}|_{\gamma_1}).\end{aligned}\tag{2.21}$$

Now we can focus on A_1 :

$$\begin{aligned}A_1 &= 2\mu \int_{-\frac{d}{2}}^{\frac{d}{2}} \nabla^n \cdot \varepsilon(\mathbf{u}_f) d\mathbf{n} \\ &= 2\mu \int_{-\frac{d}{2}}^{\frac{d}{2}} \frac{\partial}{\partial x} \left\langle \frac{\partial u_x}{\partial x}, \frac{1}{2} \left(\frac{\partial u_x}{\partial y} + \frac{\partial u_y}{\partial x} \right), \frac{1}{2} \left(\frac{\partial u_x}{\partial z} + \frac{\partial u_z}{\partial x} \right) \right\rangle d\mathbf{n}.\end{aligned}\tag{2.22}$$

In the last equation we rewrote $\nabla^n \cdot \varepsilon(\mathbf{u}_f)$ by the components, assuming that $\mathbf{n} = \langle 1, 0, 0 \rangle$. Now we can divide the vector into part with ∂x and without it:

$$\begin{aligned}A_1 &= 2\mu \int_{-\frac{d}{2}}^{\frac{d}{2}} \frac{\partial}{\partial x} \left(\frac{1}{2} \frac{\partial \mathbf{u}_f}{\partial x} + \frac{1}{2} \left\langle \frac{\partial u_x}{\partial x}, 0, 0 \right\rangle + \left\langle 0, \frac{1}{2} \frac{\partial u_x}{\partial y}, \frac{1}{2} \frac{\partial u_x}{\partial z} \right\rangle \right) d\mathbf{n} \\ &= 2\mu \int_{-\frac{d}{2}}^{\frac{d}{2}} \frac{\partial}{\partial x} \left(\frac{1}{2} \nabla^n \mathbf{u}_f + \frac{1}{2} (\nabla^n \cdot \mathbf{u}_f) \mathbf{n} + \frac{1}{2} \nabla^\tau (\mathbf{u}_f \cdot \mathbf{n}) \right) d\mathbf{n}\end{aligned}$$

This division is important because differentiation in "x - axis" direction is not defined in γ . We can use the same approximation of parts with normal divergence and normal gradient like in the case of B_2 . Expressions with tangential divergence

we just integrate.

$$A_1 \approx 2\mu_f \left(\frac{1}{2} \frac{\mathbf{u}_2|_{\gamma_2} - \mathbf{U}}{\frac{d}{2}} - \frac{1}{2} \frac{\mathbf{U} - \mathbf{u}_1|_{\gamma_1}}{\frac{d}{2}} + \frac{1}{2} \frac{(\mathbf{u}_{2,n}|_{\gamma_2} - \mathbf{U}_n)}{\frac{d}{2}} - \frac{1}{2} \frac{(\mathbf{U}_n - \mathbf{u}_{1,n}|_{\gamma_1})}{\frac{d}{2}} + \dots \right. \\ \left. \dots + \nabla^\tau \frac{\mathbf{u}_2|_{\gamma_2} \cdot \mathbf{n}}{2} - \nabla^\tau \frac{\mathbf{u}_1|_{\gamma_1} \cdot \mathbf{n}}{2} \right)$$

We already obtain the final form of A_1 :

$$A_1 \approx \mu_f \frac{2}{d} \left((\mathbf{u}_2|_{\gamma_2} - \mathbf{U}) - (\mathbf{U} - \mathbf{u}_1|_{\gamma_1}) + (\mathbf{u}_{2,n}|_{\gamma_2} - \mathbf{U}_n) - (\mathbf{U}_n - \mathbf{u}_{1,n}|_{\gamma_1}) + \dots \right. \\ \left. \dots + \frac{d}{2} (\nabla^\tau \mathbf{u}_2|_{\gamma_2} \cdot \mathbf{n}) - \frac{d}{2} (\nabla^\tau \mathbf{u}_1|_{\gamma_1} \cdot \mathbf{n}) \right). \quad (2.23)$$

We now begin with A_2 :

$$A_2 = 2\mu_f \int_{-\frac{d}{2}}^{\frac{d}{2}} \nabla^\tau \cdot \varepsilon(\mathbf{u}_f) d\mathbf{n} \\ = 2\mu_f \int_{-\frac{d}{2}}^{\frac{d}{2}} \nabla^\tau \cdot \left(\frac{\nabla^\tau \mathbf{u}_f + (\nabla^\tau \mathbf{u}_f)^T}{2} + \frac{\nabla^n \mathbf{u}_f + (\nabla^n \mathbf{u}_f)^T}{2} \right) d\mathbf{n} \\ = 2\mu_f \frac{\nabla^\tau \cdot}{2} \int_{-\frac{d}{2}}^{\frac{d}{2}} \nabla^\tau \mathbf{u}_f + (\nabla^\tau \mathbf{u}_f)^T d\mathbf{n} + 2\mu_f \frac{\nabla^\tau \cdot}{2} \int_{-\frac{d}{2}}^{\frac{d}{2}} \nabla^n \mathbf{u}_f + (\nabla^n \mathbf{u}_f)^T d\mathbf{n} \\ = \mu_f \nabla^\tau \cdot d\nabla^\tau \mathbf{U}_\tau + \mu_f \nabla^\tau \cdot d(\nabla^\tau \mathbf{U}_\tau)^T + \mu_f \nabla^\tau \cdot \int_{-\frac{d}{2}}^{\frac{d}{2}} \nabla^n \mathbf{u}_f + (\nabla^n \mathbf{u}_f)^T d\mathbf{n} \\ = \mu_f \nabla^\tau \cdot d\nabla^\tau \mathbf{U}_\tau + \mu_f \nabla^\tau \cdot d(\nabla^\tau \mathbf{U}_\tau)^T + \mu_f \nabla^\tau \cdot ((\mathbf{u}_2|_{\gamma_2} - \mathbf{u}_1|_{\gamma_1}) \otimes \mathbf{n}) + \dots \\ \dots + \mu_f \int_{-\frac{d}{2}}^{\frac{d}{2}} \underbrace{\nabla^\tau \cdot (\nabla^n \mathbf{u}_f)^T}_{=0} d\mathbf{n},$$

so that

$$A_2 = \mu_f \nabla^\tau \cdot d\nabla^\tau \mathbf{U}_\tau + \mu_f \nabla^\tau \cdot d(\nabla^\tau \mathbf{U}_\tau)^T + \mu_f (\nabla^\tau \cdot (\mathbf{u}_2|_{\gamma_2} - \mathbf{u}_1|_{\gamma_1})) \mathbf{n}. \quad (2.24)$$

Finally, we complete approximation of the second equation from Biot's model (2.16) for the fracture domain. The transformed equation is composed from parts (2.23),

(2.24), (2.20), (2.21) and its final shape is:

$$\begin{aligned}
& -\lambda_f(\nabla^\tau(\mathbf{u}_2|_{\gamma_2} - \mathbf{u}_1|_{\gamma_1}) \cdot \mathbf{n}_i) - \nabla^\tau \cdot 2d\mu_f\varepsilon^\tau(\mathbf{U}_\tau) - \dots \\
& \dots - \mu_f(\nabla^\tau \cdot (\mathbf{u}_2|_{\gamma_2} - \mathbf{u}_1|_{\gamma_1})\mathbf{n}_i) - \lambda_f d \nabla^\tau(\nabla^\tau \cdot \mathbf{U}) + \alpha_f d \nabla^\tau P + \sum_{i=1}^2 \mathbf{Q}_i = \mathbf{G}d,
\end{aligned} \tag{2.25}$$

where

$$\varepsilon^\tau(\mathbf{U}_\tau) := \frac{\nabla^\tau \mathbf{U}_\tau + (\nabla^\tau \mathbf{U}_\tau)^T}{2}, \tag{2.26a}$$

$$\mathbf{G} := \frac{1}{d} \int_{-\frac{d}{2}}^{\frac{d}{2}} \mathbf{g}, \tag{2.26b}$$

$$\begin{aligned}
\mathbf{Q}_i & := \mu_f \frac{2}{d} (\chi_i + \chi_{i,n}) + \mu_f (\nabla^\tau(\mathbf{u}_i \cdot \mathbf{n}_i)) + \dots \\
& \dots + \lambda_f \frac{2}{d} (\chi_i \cdot \mathbf{n}_i) \mathbf{n}_i + \lambda_f (\nabla^\tau \cdot \mathbf{u}_i) \mathbf{n}_i - \alpha_f (p_i \mathbf{n}_i),
\end{aligned} \tag{2.26c}$$

$$\chi_i := (\mathbf{U} - \mathbf{u}_i|_{\gamma_i}), \tag{2.26d}$$

$$\chi_{i,n} := (\mathbf{U}_n - \mathbf{u}_{i,n}|_{\gamma_i}) \quad i = 1, 2.$$

It remains to replace the interface condition (2.4) in terms of P and \mathbf{U} . Similarly as in (2.11) one can write:

$$\mathbb{K} \nabla p_i \cdot \mathbf{n}_i \approx k \frac{P - p_i|_{\gamma_i}}{d/2} := Q_i \quad \text{on } (0, T) \times \gamma_i, \quad i = 1, 2, \tag{2.27}$$

where \mathbf{n}_i denotes the normal vector on $\partial\Omega_i$ pointing out of Ω_i . The conditions for the poroelastic stress read:

$$\mathbb{C}\varepsilon(\mathbf{u}_i)\mathbf{n}_i - \alpha p_i \mathbf{n}_i \approx \mathbf{Q}_i \quad \text{on } \gamma_i \quad i = 1, 2. \tag{2.28}$$

We can write our approximated Biot's system together with all boundary conditions. Our system contains the following equations for the unknowns $(p_1, p_2, P, \mathbf{u}_1, \mathbf{u}_2, \mathbf{U})$:

$$\partial_t(Sp_i + \alpha \nabla \cdot \mathbf{u}_i) - \nabla \cdot (\mathbb{K} \nabla p_i) = f \quad \text{in } (0, T) \times \Omega_i, \quad i = 1, 2 \tag{2.29a}$$

$$-\nabla \cdot (\mathbb{C}\varepsilon(\mathbf{u}_i) - \alpha p_i \mathbf{I}) = \mathbf{g} \quad \text{in } (0, T) \times \Omega_i, \quad i = 1, 2 \tag{2.29b}$$

$$\begin{aligned}
& d\left(\partial_t \left[S P + \alpha_f \nabla^\tau \cdot \mathbf{U} \right] - \nabla^\tau \cdot (\mathbb{K}_{f,\tau} \nabla^\tau P)\right) + \dots \\
& \dots + \alpha_f \partial_t (\mathbf{u}_2|_{\gamma_2} - \mathbf{u}_1|_{\gamma_1}) \cdot \mathbf{n} + \sum_{i=1}^2 Q_i = Fd \quad \text{in} \quad (0, T) \times \gamma
\end{aligned} \tag{2.29c}$$

$$\begin{aligned}
& - \lambda_f \nabla^\tau \left((\mathbf{u}_2|_{\gamma_2} - \mathbf{u}_1|_{\gamma_1}) \cdot \mathbf{n} \right) - \nabla^\tau \cdot 2d\mu_f \varepsilon^\tau(\mathbf{U}_\tau) - \dots \\
& \dots - \mu_f (\nabla^\tau \cdot (\mathbf{u}_2|_{\gamma_2} - \mathbf{u}_1|_{\gamma_1})) \mathbf{n} - \lambda_f d \nabla^\tau (\nabla^\tau \cdot \mathbf{U}) + \alpha_f d \nabla^\tau P + \dots \\
& \dots + \sum_{i=1}^2 \mathbf{Q}_i = \mathbf{G}d \quad \text{in} \quad (0, T) \times \gamma.
\end{aligned} \tag{2.29d}$$

Let us denote:

$$\Gamma_i := \partial\Omega_i \cap \partial\Omega, \quad i = 1, 2.$$

Then we also consider the boundary conditions

$$p_i = 0, \quad \mathbf{u}_i = \mathbf{0} \quad \text{on} \quad (0, T) \times \Gamma_i, \tag{2.29e}$$

$$P = 0, \quad \mathbf{U} = \mathbf{0} \quad \text{on} \quad (0, T) \times \partial\gamma \tag{2.29f}$$

$$\mathbb{C} \varepsilon(\mathbf{u}_i) \mathbf{n}_i - \alpha p_i \mathbf{n}_i = \mathbf{Q}_i \quad \text{on} \quad (0, T) \times \gamma_i \quad i = 1, 2, \tag{2.29g}$$

$$\mathbb{K} \nabla p_i \cdot \mathbf{n}_i = Q_i \quad \text{on} \quad (0, T) \times \gamma_i, \quad i = 1, 2, \tag{2.29h}$$

and the initial conditions

$$p_i(0, \cdot) = p_0 \quad \text{in} \quad \Omega_i, \quad i = 1, 2, \tag{2.29i}$$

$$P(0, \cdot) = P_0 := \frac{1}{d} \int_{-\frac{d}{2}}^{\frac{d}{2}} p_0 d\mathbf{n} \quad \text{in} \quad \gamma. \tag{2.29j}$$

2.2 Weak form

We need to find the weak form of our system (2.29) which will be useful for later numeric simulation. Our approximated system contains couple of equations, we derive weak formulation separately for each of equations. Let us define the spaces:

$$\begin{aligned}
H_{\Gamma_i}^1(\Omega_i) & := \{w \in H^1(\Omega_i); w|_{\Gamma_i} = 0\}, \quad i = 1, 2, \\
H_0^1(\gamma) & := \{w_f \in H^1(\gamma); w_f|_{\partial\gamma} = 0\},
\end{aligned} \tag{2.30}$$

where $H^1(M)$ stands for Sobolev space on domain M . We define the space \mathbb{V} :

$$\mathbb{V} := H_{\Gamma_1}^1(\Omega_1) \times H_{\Gamma_2}^1(\Omega_2) \times H_0^1(\gamma) \times (H_{\Gamma_1}^1(\Omega_1))^n \times (H_{\Gamma_2}^1(\Omega_2))^n \times (H_0^1(\gamma))^n. \quad (2.31)$$

The weak solution of (2.29) is the sextuple $(p_1, p_2, P, \mathbf{u}_1, \mathbf{u}_2, \mathbf{U}) \in C^1([0, T]; \mathbb{V})$, continuously differentiable in time with values in \mathbb{V} , and satisfying the equations, initial and boundary conditions in a weak sense. In what follows we derive the appropriate linear and bilinear forms. We start with finding a weak form of Darcy's equation (2.29a) for the bulk spaces Ω_1, Ω_2 . We multiply the equations by scalar test functions $w_i \in H_{\Gamma_i}^1(\Omega_i)$, integrate and sum:

$$\sum_{i=1}^2 \int_{\Omega_i} \partial_t (S p_i + \alpha \nabla \cdot \mathbf{u}_i) w_i - \sum_{i=1}^2 \int_{\Omega_i} (\nabla \cdot (\mathbb{K}_i \nabla p_i)) w_i = \sum_{i=1}^2 \int_{\Omega_i} f_i w_i.$$

Applying the Green theorem to the second term we obtain:

$$\begin{aligned} \sum_{i=1}^2 \partial_t \int_{\Omega_i} (S p_i + \alpha \nabla \cdot \mathbf{u}_i) w_i - \sum_{i=1}^2 \int_{\partial\Omega_i} ((\mathbb{K}_i \nabla p_i) \cdot \mathbf{n}_i) w_i + \dots \\ \dots + \sum_{i=1}^2 \int_{\Omega_i} (\mathbb{K}_i \nabla p_i) \cdot \nabla w_i = \sum_{i=1}^2 \int_{\Omega_i} f_i w_i. \end{aligned} \quad (2.32)$$

We need to divide boundary of bulk spaces $\partial\Omega$ into four parts. The whole boundary consists of exterior boundaries Γ_1, Γ_2 and the fracture boundaries γ_1, γ_2 . Then the boundary integral in (2.32) can be rewritten as follows:

$$\sum_{i=1}^2 \int_{\partial\Omega_i} ((\mathbb{K}_i \nabla p_i) \cdot \mathbf{n}_i) w_i = \sum_{i=1}^2 \int_{\Gamma_i} ((\mathbb{K}_i \nabla p_i) \cdot \mathbf{n}_i) w_i + \sum_{i=1}^2 \int_{\gamma_i} ((\mathbb{K}_i \nabla p_i) \cdot \mathbf{n}_i) w_i.$$

On the exterior boundaries we have defined zero Dirichlet condition, then parts which are integrated along Γ_1, Γ_2 can be skipped. The term on γ_i is replaced from (2.29h), hence (2.32) becomes:

$$\sum_{i=1}^2 \partial_t \int_{\Omega_i} (S p_i + \alpha \nabla \cdot \mathbf{u}_i) w_i - \sum_{i=1}^2 \int_{\gamma_i} Q_i w_i + \sum_{i=1}^2 \int_{\Omega_i} (\mathbb{K}_i \nabla p_i) \cdot \nabla w_i = \sum_{i=1}^2 \int_{\Omega_i} f_i w_i, \quad (2.33)$$

where $Q_i := Q_i(p_i, P)$ is defined in (2.27). We introduce the following variational forms:

$$\begin{aligned}
D_1(\mathbf{u}_1, p_1, w_1, P) &= - \int_{\gamma_1} Q_1 w_1 + \int_{\Omega_1} (\mathbb{K}_1 \nabla p_1) \cdot \nabla w_1, \\
D_{t,1}(\mathbf{u}_1, p_1, w_1) &= \partial_t \int_{\Omega_1} (S p_1 + \alpha \nabla \cdot \mathbf{u}_1) w_1 \\
L_{D1}(w_1) &= \int_{\Omega_1} f_1 w_1. \\
D_2(\mathbf{u}_2, p_2, w_2, P) &= - \int_{\gamma} Q_2 w_2 + \int_{\Omega_2} (\mathbb{K}_2 \nabla p_2) \cdot \nabla w_2, \\
D_{t,2}(\mathbf{u}_2, p_2, w_2) &= \partial_t \int_{\Omega_2} (S p_2 + \alpha \nabla \cdot \mathbf{u}_2) w_2 \\
L_{D2}(w_2) &= \int_{\Omega_2} f_2 w_2.
\end{aligned} \tag{2.34}$$

Now, we can move our attention on approximated Darcy's equation (2.29), which is defined on reduced fracture space γ . We will use test function $w_f \in H_0^1(\gamma)$. After using Green's theorem, weak form of the equation (2.15) is:

$$\begin{aligned}
& d \partial_t \int_{\gamma} (S P) w_f + d \alpha_f \partial_t \int_{\gamma} (\nabla^\tau \cdot \mathbf{U}) w_f - d \int_{\partial\gamma} (\mathbb{K}_{f,\tau} \nabla^\tau P \cdot \mathbf{n}) w_f + \dots \\
& \dots + d \int_{\gamma} (\mathbb{K}_{f,\tau} \nabla^\tau P) \cdot \nabla^\tau w_f + \alpha_f \partial_t \int_{\gamma} ((\mathbf{u}_2|_{\gamma_2} - \mathbf{u}_1|_{\gamma_1}) \cdot \mathbf{n}) w_f - \sum_{i=1}^2 \int_{\gamma} Q_i w_f = d \int_{\gamma} F w_f
\end{aligned}$$

From the definition of the test function w_f we know that it is zero on boundary $\partial\gamma$, then we obtain this expression for the weak form:

$$\begin{aligned}
& d \partial_t \int_{\gamma} (S P) w_f + d \alpha_f \partial_t \int_{\gamma} (\nabla^\tau \cdot \mathbf{U}) w_f + d \int_{\gamma} (\mathbb{K}_{f,\tau} \nabla^\tau P) \cdot \nabla^\tau w_f + \dots \\
& \dots + \alpha_f \partial_t \int_{\gamma} ((\mathbf{u}_2|_{\gamma_2} - \mathbf{u}_1|_{\gamma_1}) \cdot \mathbf{n}) w_f + \sum_{i=1}^2 \int_{\gamma} Q_i w_f = d \int_{\gamma} F w_f
\end{aligned} \tag{2.35}$$

The corresponding variational forms are:

$$\begin{aligned}
D_f(\mathbf{u}_1, \mathbf{u}_2, p_1, p_2, U, P, w_f) &= d \int_{\gamma} (\mathbb{K}_{f,\tau} \nabla^\tau P) \cdot \nabla^\tau w_f + \sum_{i=1}^2 \int_{\gamma} Q_i w_f \\
D_{f,t}(\mathbf{u}_1, \mathbf{u}_2, U, P, w_f) &= d \partial_t \int_{\gamma} (S P) w_f + d \alpha_f \partial_t \int_{\gamma} (\nabla^\tau \cdot \mathbf{U}) w_f + \dots \\
&\dots + \alpha_f \partial_t \int_{\gamma} ((\mathbf{u}_2|_{\gamma_2} - \mathbf{u}_1|_{\gamma_1}) \cdot \mathbf{n}) w_f, \\
L_{Df}(w_f) &= d \int_{\gamma} F w_f.
\end{aligned} \tag{2.36}$$

Earlier, we mentioned that we need the weak form for all equations from system (2.29). We already obtained full weak form of Darcy's equation (2.1). Now, we start to derive the weak form of the *elasticity* equation (2.29b) for the bulk spaces Ω_1, Ω_2 with test functions $\mathbf{r}_i \in (H_{\Gamma_i}^1(\Omega_i))^n$, $i = 1, 2$.

$$-\sum_{i=1}^2 \int_{\Omega_i} \nabla \cdot (\mathbb{C}\varepsilon(\mathbf{u}_i) - \alpha(p_i \mathbb{I})) \cdot \mathbf{r}_i = \sum_{i=1}^2 \int_{\Omega_i} \mathbf{g}_i \cdot \mathbf{r}_i. \tag{2.37}$$

We can again use the Green theorem and also we have to divide boundaries because of boundary conditions. After using Dirichlet condition on boundaries Γ_1, Γ_2 we gain this expression:

$$\begin{aligned}
&-\sum_{i=1}^2 \int_{\gamma_i} (\mathbb{C}\varepsilon(\mathbf{u}_i) \mathbf{n}_i) \cdot \mathbf{r}_i + \sum_{i=1}^2 \int_{\Omega_i} (\mathbb{C}\varepsilon(\mathbf{u}_i)) \cdot \nabla \mathbf{r}_i + \dots \\
&\dots + \alpha \sum_{i=1}^2 \int_{\gamma_i} p_i \mathbf{n}_i \cdot \mathbf{r}_i - \alpha \sum_{i=1}^2 \int_{\Omega_i} (p_i \mathbb{I}) \cdot \nabla \mathbf{r}_i = \sum_{i=1}^2 \int_{\Omega_i} \mathbf{g}_i \cdot \mathbf{r}_i.
\end{aligned} \tag{2.38}$$

It is possible to replace the first and the third expression of this equation on the base of the boundary condition (2.29g):

$$-\sum_{i=1}^2 \int_{\gamma_i} \mathbf{Q}_i \cdot \mathbf{r}_i + \sum_{i=1}^2 \int_{\Omega_i} (\mathbb{C}\varepsilon(\mathbf{u}_i)) \cdot \nabla \mathbf{r}_i - \alpha \sum_{i=1}^2 \int_{\Omega_i} p_i \nabla \cdot \mathbf{r}_i = \sum_{i=1}^2 \int_{\Omega_i} \mathbf{g}_i \cdot \mathbf{r}_i. \tag{2.39}$$

Here $\mathbf{Q}_i := \mathbf{Q}_i(\mathbf{u}_i, U, p_i)$ is defined in (2.26c) We also define variational forms for

equation of elasticity in bulk domains:

$$\begin{aligned}
E_1(\mathbf{u}_1, p_1, \mathbf{r}_1, \mathbf{U}) &= - \int_{\gamma_1} \mathbf{Q}_1 \cdot \mathbf{r}_1 + \int_{\Omega_1} (\mathbb{C}\varepsilon(\mathbf{u}_1)) \cdot \nabla \mathbf{r}_1 - \alpha \int_{\Omega_1} p_1 \nabla \cdot \mathbf{r}_1, \\
L_{E1}(\mathbf{r}_1) &= \int_{\Omega_1} \mathbf{g}_1 \cdot \mathbf{r}_1, \\
E_2(\mathbf{u}_2, p_2, \mathbf{r}_2, \mathbf{U}) &= - \int_{\gamma_2} \mathbf{Q}_2 \cdot \mathbf{r}_2 + \int_{\Omega_2} (\mathbb{C}\varepsilon(\mathbf{u}_2)) \cdot \nabla \mathbf{r}_2 - \int_{\Omega_2} p_2 \nabla \cdot \mathbf{r}_2, \\
L_{E2}(\mathbf{r}_2) &= \int_{\Omega_2} \mathbf{g}_2 \cdot \mathbf{r}_2.
\end{aligned} \tag{2.40}$$

For obtaining the weak form of the elasticity equation in fracture we will need to make little bit more effort. Multiplying (2.29d) by a test function $\mathbf{r}_f \in (H_0^1(\gamma))^n$ and integrating we get:

$$\begin{aligned}
& - \lambda_f \underbrace{\int_{\gamma} \nabla^\tau ((\mathbf{u}_2|_{\gamma_2} - \mathbf{u}_1|_{\gamma_1}) \cdot \mathbf{n}) \cdot \mathbf{r}_f}_{(I)} - 2d \mu_f \underbrace{\int_{\gamma} (\nabla^\tau \cdot \varepsilon^\tau(\mathbf{U}_\tau)) \cdot \mathbf{r}_f}_{(II)} - \dots \\
& \dots - \mu_f \underbrace{\int_{\gamma} (\nabla^\tau \cdot (\mathbf{u}_2|_{\gamma_2} - \mathbf{u}_1|_{\gamma_1})) \mathbf{n} \cdot \mathbf{r}_f}_{(III)} - \lambda_f d \underbrace{\int_{\gamma} \nabla^\tau (\nabla^\tau \cdot \mathbf{U}) \cdot \mathbf{r}_f}_{(IV)} + \alpha_f d \underbrace{\int_{\gamma} (\nabla^\tau P) \cdot \mathbf{r}_f}_{(V)} + \dots \\
& \dots + \sum_{i=1}^2 \int_{\gamma} \mathbf{Q}_i \cdot \mathbf{r}_f = d \int_{\gamma} \mathbf{G} \cdot \mathbf{r}_f.
\end{aligned} \tag{2.41}$$

Like before, we can use Green's theorem in the expressions (I – V).

$$\begin{aligned}
(I) &= \int_{\partial\gamma} ((\mathbf{u}_2|_{\gamma_2} - \mathbf{u}_1|_{\gamma_1}) \cdot \mathbf{n})(\mathbf{r}_f \cdot \mathbf{n}_\gamma) - \int_{\gamma} ((\mathbf{u}_2|_{\gamma_2} - \mathbf{u}_1|_{\gamma_1}) \cdot \mathbf{n})(\nabla^\tau \cdot \mathbf{r}_f) \\
(II) &= \int_{\partial\gamma} (\varepsilon^\tau(\mathbf{U}_\tau) \mathbf{n}_\gamma) \cdot \mathbf{r}_f - \int_{\gamma} \varepsilon^\tau(\mathbf{U}_\tau) \cdot \varepsilon^\tau \mathbf{r}_f \\
(III) &= \int_{\partial\gamma} ((\mathbf{u}_2|_{\gamma_2} - \mathbf{u}_1|_{\gamma_1}) \cdot \mathbf{n}_\gamma)(\mathbf{r}_f \cdot \mathbf{n}) - \int_{\gamma} (\mathbf{u}_2|_{\gamma_2} - \mathbf{u}_1|_{\gamma_1}) \cdot \varepsilon^\tau(\mathbf{r}_f \cdot \mathbf{n}) \\
(IV) &= \int_{\partial\gamma} (\nabla^\tau \cdot \mathbf{U})(\mathbf{r}_f \cdot \mathbf{n}_\gamma) - \int_{\gamma} (\nabla^\tau \cdot \mathbf{U})(\nabla^\tau \cdot \mathbf{r}_f) \\
(V) &= \int_{\partial\gamma} P(\mathbf{r}_f \cdot \mathbf{n}_\gamma) - \int_{\gamma} P(\nabla^\tau \cdot \mathbf{r}_f)
\end{aligned} \tag{2.42}$$

In (2.42), all integrals over $\partial\gamma$ vanish due to the boundary condition (2.29f). The

weak form of the elasticity equation in fracture is:

$$\begin{aligned}
& \lambda_f \int_{\gamma} ((\mathbf{u}_2|_{\gamma_2} - \mathbf{u}_1|_{\gamma_1}) \cdot \mathbf{n})(\nabla^\tau \cdot \mathbf{r}_f) + 2d\mu_f \int_{\gamma} \varepsilon^\tau(\mathbf{U}_\tau) \cdot \varepsilon^\tau \mathbf{r}_f + \dots \\
& \dots + \mu_f \int_{\gamma} (\mathbf{u}_2|_{\gamma_2} - \mathbf{u}_1|_{\gamma_1}) \cdot \nabla^\tau(\mathbf{r}_f \cdot \mathbf{n}) + \lambda_f d \int_{\gamma} (\nabla^\tau \cdot \mathbf{U})(\nabla^\tau \cdot \mathbf{r}_f) - \dots \quad (2.43) \\
& \dots - \alpha_f d \int_{\gamma} P(\nabla^\tau \cdot \mathbf{r}_f) + \sum_{i=1}^2 \int_{\gamma} \mathbf{Q}_i \cdot \mathbf{r}_f = d \int_{\gamma} \mathbf{G} \cdot \mathbf{r}_f.
\end{aligned}$$

The corresponding forms are:

$$\begin{aligned}
E_f(\mathbf{u}_1, \mathbf{u}_2, \mathbf{r}_f, P, \mathbf{U}) &= \lambda_f \int_{\gamma} ((\mathbf{u}_2|_{\gamma_2} - \mathbf{u}_1|_{\gamma_1}) \cdot \mathbf{n})(\nabla^\tau \cdot \mathbf{r}_f) + 2d\mu_f \int_{\gamma} \varepsilon^\tau(\mathbf{U}_\tau) \cdot \varepsilon^\tau \mathbf{r}_f + \dots \\
& \dots + \mu_f \int_{\gamma} (\mathbf{u}_2|_{\gamma_2} - \mathbf{u}_1|_{\gamma_1}) \cdot \nabla^\tau(\mathbf{r}_f \cdot \mathbf{n}) + \lambda_f d \int_{\gamma} (\nabla^\tau \cdot \mathbf{U})(\nabla^\tau \cdot \mathbf{r}_f) - \dots \\
& \dots - \alpha_f d \int_{\gamma} P(\nabla^\tau \cdot \mathbf{r}_f) + \sum_{i=1}^2 \int_{\gamma} \mathbf{Q}_i \cdot \mathbf{r}_f \\
L_{E_f}(\mathbf{r}_f) &= d \int_{\gamma} \mathbf{G} \cdot \mathbf{r}_f.
\end{aligned} \quad (2.44)$$

Then the variational formulation is the following:

Weak formulation of (2.29)

Find a sextuple $\mathbf{s} := (p_1, p_2, P, \mathbf{u}_1, \mathbf{u}_2, \mathbf{U}) \in C^1([0, T]; \mathbb{V})$ such that:

$$\begin{aligned}
(i) \quad & (p_1, p_2, P)(0, \cdot) = (p_0|_{\Omega_1}, p_0|_{\Omega_2}, P_0), \quad (2.45) \\
(ii) \quad & \forall \mathbf{t} := (w_1, w_2, w_f, \mathbf{r}_1, \mathbf{r}_2, \mathbf{r}_f) \in \mathbb{V}, \forall t \in (0, T) : \\
& a_t(\mathbf{s}(t), \mathbf{t}) + a(\mathbf{s}(t), \mathbf{t}) = l(\mathbf{t}),
\end{aligned}$$

where

$$\begin{aligned}
a_t((p_1, p_2, P, \mathbf{u}_1, \mathbf{u}_2, \mathbf{U}), (w_1, w_2, w_f, \mathbf{r}_1, \mathbf{r}_2, \mathbf{r}_f)) &:= D_{1,t}(\mathbf{u}_1, p_1, w_1) + \dots \\
&\dots + D_{2,t}(\mathbf{u}_2, p_2, w_2) + D_{f,t}(p_1, p_2, P, w_f), \\
a((p_1, p_2, P, \mathbf{u}_1, \mathbf{u}_2, \mathbf{U}), (w_1, w_2, w_f, \mathbf{r}_1, \mathbf{r}_2, \mathbf{r}_f)) &:= D_1(\mathbf{u}_1, p_1, w_1, P) + \dots \\
&\dots + D_2(\mathbf{u}_2, p_2, w_2, P) + D_f(\mathbf{u}_1, \mathbf{u}_2, p_1, p_2, \mathbf{U}, P, w_f) + \dots \\
&\dots + E_1(\mathbf{u}_1, p_1, \mathbf{r}_1, \mathbf{U}) + E_2(\mathbf{u}_2, p_2, \mathbf{r}_2, \mathbf{U}) + E_f(\mathbf{u}_1, \mathbf{u}_2, \mathbf{r}_f, P, \mathbf{U}), \\
l(w_1, w_2, w_f, \mathbf{r}_1, \mathbf{r}_2, \mathbf{r}_f) &:= L_{D1}(w_1) + L_{D2}(w_2) + \dots \\
&\dots + L_{Df}(w_f) + L_{E1}(\mathbf{r}_1) + L_{E2}(\mathbf{r}_2) + L_{Ef}(\mathbf{r}_f).
\end{aligned}$$

Chapter 3

Numerical solution

The aim of this chapter is to solve the system (2.29). Like almost all other systems of PDEs, also for our modified Biot's system the analytical solution is in general impossible. Due to unknown analytical solution, we try to find a numerical solution, at least.

3.1 Time and space discretization

Our numerical method requires discretization of the weak formulation of (2.29). Our problem consists of 2 bulk subdomains Ω_1 , Ω_2 what need to be discretized and one line interface γ between them. We shall first describe the approximation in space and later in time.

3.1.1 Space discretization

We try to find the numerical solution with help of the *Finite element method (FEM)*. It is a widespread method for simulation of various physical problems like structural analysis, linear elasticity, etc. The base of FEM lies in dividing the computational domain into many small pieces. On this subdivision we introduce the finite element space of continuous piecewise polynomials of certain degree. In the previous chapter, we mentioned that the domain Ω consists of 3 subregions, see (2.3). We assume that the domains $\bar{\Omega}_i$, $i = 1, 2$ are unions of finite number of disjoint *elements* $\bar{\Omega}_i = \cup_{E \in \mathcal{T}_{h,i}} E$. Here $\mathcal{T}_{h,i}$ is called a triangulation (*mesh*) of the bulk domain (Ω_i) and h is the diameter of the largest element in the sets $\mathcal{T}_{h,i}$, $i = 1, 2$. All *elements* E in the bulk domains are the *simplexes*. In what follows,

we consider only two-dimensional problem, hence the elements will be triangles. We also introduce a finite element approximation for the reduced subdomain $\bar{\gamma} = \cup_{E \in \mathcal{T}_{h,f}} E$. The cells (elements) in the interface γ have to be lower dimensional simplices, in our case lines. We will use conforming meshes of Ω_1 , Ω_2 and γ ,

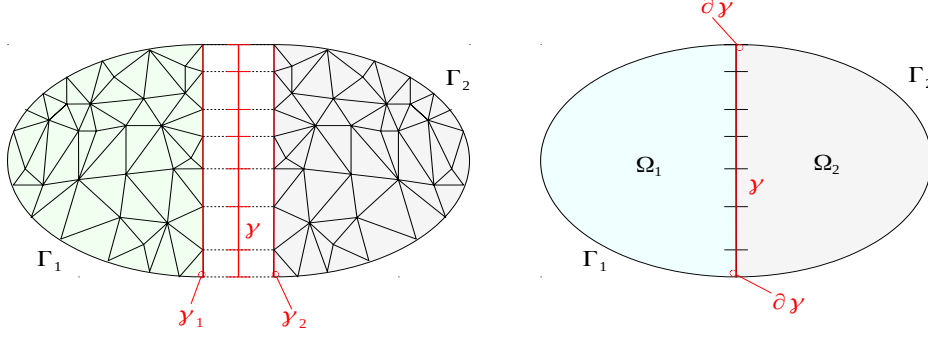


Figure 3.1: *Conforming meshing, (Left): Two-dimensional domain Ω with a simplex mesh. (Right): The one-dimensional reduced fracture γ is meshed with the line segments.*

i.e. such that the elements of $\mathcal{T}_{h,f}$ are faces of some elements of $\mathcal{T}_{h,1}$ and of $\mathcal{T}_{h,2}$, see Figure 3.1. We define the spaces $\mathbb{P}_{h,i}^k$ and $\mathbb{P}_{h,f}^k$ of continuous piecewise polynomial of degree k :

$$\begin{aligned} \mathbb{P}_{h,i}^k &:= \{\varphi \in C(\bar{\Omega}_i); \forall E \in \mathcal{T}_{h,i}, \varphi|_E \text{ is polynomial of degree } \leq k\}, \quad i = 1, 2, \\ \mathbb{P}_{h,f}^k &:= \{\varphi \in C(\bar{\gamma}); \forall E \in \mathcal{T}_{h,f}, \varphi|_E \text{ is polynomial of degree } \leq k\}. \end{aligned}$$

Let us define the discrete spaces

$$\begin{aligned} \mathbb{W}_{h,1} &:= (H_{\Gamma_1}^1(\Omega_1) \cap \mathbb{P}_{h,1}^k) \\ \mathbb{W}_{h,2} &:= (H_{\Gamma_2}^1(\Omega_2) \cap \mathbb{P}_{h,2}^k) \\ \mathbb{W}_{h,f} &:= (H_0^1(\gamma) \cap \mathbb{P}_{h,f}^k), \end{aligned}$$

and the space for the finite element solution:

$$\mathbb{V}_h := \mathbb{W}_{h,1} \times \mathbb{W}_{h,2} \times \mathbb{W}_{h,f} \times (\mathbb{W}_{h,1})^n \times (\mathbb{W}_{h,2})^n \times (\mathbb{W}_{h,f})^n.$$

Instead of solving the variational problem (2.45), we will solve Galerkin's discrete

problem:

Find a sextuple $\mathbf{s}_h := (p_{h,1}, p_{h,2}, P_h, \mathbf{u}_{h,1}, \mathbf{u}_{h,2}, \mathbf{U}_h) \in C^1([0, T]; \mathbb{V}_h)$ such that :

$$(i) \quad (p_{h,1}, p_{h,2}, P)(0, \cdot) = (\tilde{p}_0|_{\Omega_1}, \tilde{p}_0|_{\Omega_2}, \tilde{P}_0),$$

where $\tilde{\cdot}$ denotes the projection onto the respective finite element space.

$$(ii) \quad \forall \mathbf{t}_h (w_{h,1}, w_{h,2}, w_{h,f}, \mathbf{r}_{h,1}, \mathbf{r}_{h,2}, \mathbf{r}_{h,f}) \in \mathbb{V}_h, \forall t \in (0, T) :$$

$$a_t(\mathbf{s}_h(t), \mathbf{t}_h) + a(\mathbf{s}_h(t), \mathbf{t}) = l(\mathbf{l}).$$

(3.1)

3.1.2 Time discretization

As before we divide time discretization of system the weak formulation of (2.29) into several parts. We will discretize each equation separately using appropriate linear and bilinear forms. We will divide the time interval $[0, T]$ to equidistant time steps:

$$\Delta t = \frac{T}{N}, \quad (3.2)$$

where Δt refers to the length of the time step and N is the number of time steps. Approximation of the time derivative ($\frac{\partial}{\partial t}$) is made by the simple *implicit Euler method*:

$$\partial_t \Phi(t) \approx \frac{\Phi(t) - \Phi(t - \Delta t)}{\Delta t}. \quad (3.3)$$

We start to approximate the weak form of the Darcy equation (2.33) for bulk spaces. It means we replace the time derivative by a *finite difference* according to (3.3) and we will find solution only for discrete time steps $t = \Delta t, 2\Delta t, 3\Delta t, \dots, T$. Let the superscript j denote a quantity at time $t_j := j\Delta t$, where j is an integer counting time levels. For example, u^j means u at time level t_j . A finite difference discretization in time first consists of sampling the PDE at some time level, say t_j :

$$\begin{aligned} \partial_t \left(\sum_{i=1}^2 \int_{\Omega_i} (S p_i + \alpha \nabla \cdot \mathbf{u}_i) w_i \right)^j - \left(\sum_{i=1}^2 \int_{\gamma_i} Q_i w_i \right)^j + \dots \\ \dots + \left(\sum_{i=1}^2 \int_{\Omega_i} (\mathbb{K}_i \nabla p_i) \cdot \nabla w_i \right)^j = \left(\sum_{i=1}^2 \int_{\Omega_i} f_i w_i \right)^j. \end{aligned} \quad (3.4)$$

The time-derivative in (3.4) is replaced by simple backward difference:

$$\left(\int_{\Omega_i} (S p_i + \alpha \nabla \cdot \mathbf{u}_i) w_i \right)^j \approx \frac{\left(\int_{\Omega_i} (S p_i + \alpha \nabla \cdot \mathbf{u}_i) w_i \right)^j - \left(\int_{\Omega_i} (S p_i + \alpha \nabla \cdot \mathbf{u}_i) w_i \right)^{j-1}}{\Delta t}. \quad (3.5)$$

We assume that only functions p_i , \mathbf{u}_i , Q_i , f are time-dependent. In accordance with to this assumption we can rewrite equation (3.4) into the form:

$$\begin{aligned} & \frac{1}{\Delta t} \sum_{i=1}^2 \int_{\Omega_i} (S p_i^j + \alpha \nabla \cdot \mathbf{u}_i^j) w_i - \frac{1}{\Delta t} \sum_{i=1}^2 \int_{\Omega_i} (S p_i^{j-1} + \alpha \nabla \cdot \mathbf{u}_i^{j-1}) w_i - \dots \\ & \dots - \sum_{i=1}^2 \int_{\gamma_i} Q_i^j w_i + \sum_{i=1}^2 \int_{\Omega_i} (\mathbb{K}_i \nabla p_i^j) \cdot \nabla w_i = \sum_{i=1}^2 \int_{\Omega_i} f_i^j w_i. \end{aligned} \quad (3.6)$$

We obtained an *implicit scheme* where the solution at the current time level (t_j) is computed from the previous level (t_{j-1}). Now we continue with time discretization of the weak form (2.35). This weak form of the Darcy equation in the fracture domain contains several time-dependent unknowns. Except for p_i , \mathbf{u}_i , Q_i , f , also the new unknowns \mathbf{U} , P are time-dependent. At time level t_j we have:

$$\begin{aligned} & \partial_t d \int_{\gamma} (S P^j + \alpha_f \nabla^\tau \cdot \mathbf{U}^j) w_f + \int_{\gamma} (\mathbb{K}_{f,\tau} \nabla^\tau P^j) \cdot \nabla w_f + \dots \\ & \dots + \alpha_f \partial_t \int_{\gamma} ((\mathbf{u}_2^j|_{\gamma_2} - \mathbf{u}_1^j|_{\gamma_1}) \cdot \mathbf{n}) w_f + \sum_{i=1}^2 \int_{\gamma} Q_i^j w_f = d \int_{\gamma} F^j w_f. \end{aligned}$$

Again, we use *implicit Euler's method* for the approximation time-differentiation:

$$\begin{aligned} & \frac{d}{\Delta t} \int_{\gamma} (S P^j + \alpha_f \nabla^\tau \cdot \mathbf{U}^j) w_f + \int_{\gamma} (\mathbb{K}_{f,\tau} \nabla^\tau P^j) \cdot \nabla w_f + \dots \\ & \dots + \frac{d}{\Delta t} \alpha_f \int_{\gamma} ((\mathbf{u}_2^j|_{\gamma_2} - \mathbf{u}_1^j|_{\gamma_1}) \cdot \mathbf{n}) w_f + \sum_{i=1}^2 \int_{\gamma} Q_i^j w_f - \dots \\ & \dots - \frac{d}{\Delta t} \int_{\gamma} (S P^{j-1} + \alpha_f \nabla^\tau \cdot \mathbf{U}^{j-1}) w_f - \dots \\ & \dots - \frac{d}{\Delta t} \alpha_f \int_{\gamma} ((\mathbf{u}_2^{j-1}|_{\gamma_2} - \mathbf{u}_1^{j-1}|_{\gamma_1}) \cdot \mathbf{n}) w_f = d \int_{\gamma} F^j w_f. \end{aligned} \quad (3.7)$$

Now, the time discretization of Darcy's equation is done for all subregions. The equations of elasticity (2.29b), (2.29d) are not time-dependent. We already

discretized the whole system (2.29) in space and now also in time. Let us introduce the following forms:

$$\begin{aligned}
D_{\Delta t, i}(\mathbf{u}_i, p_i, w_i) &:= \frac{1}{\Delta t} \int_{\Omega_i} (Sp_i + \alpha \nabla \cdot \mathbf{u}_i) w_i, \quad i = 1, 2, \\
D_{\Delta t, f}(\mathbf{u}_1, \mathbf{u}_2, \mathbf{U}, P, w_f) &:= \frac{d}{\Delta t} \int_{\gamma} (SP + \alpha_f \nabla^\tau \cdot \mathbf{U}) w_f + \dots \\
&\dots + \frac{d}{\Delta t} \alpha_f \int_{\gamma} ((\mathbf{u}_2|_{\gamma_2} - \mathbf{u}_1|_{\gamma_1}) \cdot \mathbf{n}) w_f.
\end{aligned}$$

Then the final form of the discrete problems reads:

Find the sequence $\{\mathbf{s}^j\}_{j=0}^N$, $\mathbf{s}^j := (p_1^j, p_2^j, P^j, \mathbf{u}_1^j, \mathbf{u}_2^j, \mathbf{U}^j) \in \mathbb{V}_h$ such that :

(i) $(p_1^0, p_2^0, P^0) = (\mathbf{p}_0|_{\Omega_1}, \mathbf{p}_0|_{\Omega_2}, \mathbf{P}_0)$

(ii) $\forall (\mathbf{r}_1, \mathbf{r}_2, \mathbf{r}_f) \in (\mathbb{W}_{h,1})^n \times (\mathbb{W}_{h,2})^n \times (\mathbb{W}_{h,f})^n :$

$$\begin{aligned}
&E_1(\mathbf{u}_1^0, p_1^0, \mathbf{r}_1, \mathbf{U}^0) + E_2(\mathbf{u}_2^0, p_2^0, \mathbf{r}_2, \mathbf{U}^0) + \dots \\
&\dots + E_f(\mathbf{u}_1^0, \mathbf{u}_2^0, \mathbf{r}_f, P^0, \mathbf{U}^0) = L_{E_2}(\mathbf{r}_2) + L_{E_f}(\mathbf{r}_f),
\end{aligned}$$

(iii) $\forall j = 1, 2, \dots, N \quad \forall \mathbf{t} := (w_1, w_2, w_f, \mathbf{r}_1, \mathbf{r}_2, \mathbf{r}_f) \in \mathbb{V}_h :$

$$\begin{aligned}
&D_{\Delta t, 1}(\mathbf{u}_1^j, p_1^j, w_1) + D_{\Delta t, 2}(\mathbf{u}_2^j, p_2^j, w_2) + D_{\Delta t, f}(\mathbf{u}_1^j, \mathbf{u}_2^j, \mathbf{U}^j, P^j, w_f) + \dots \\
&\dots + a(\mathbf{s}^j, \mathbf{t}) = l(\mathbf{t}) + D_{\Delta t, 1}(\mathbf{u}_1^{j-1}, p_1^{j-1}, w_1) + \dots \\
&\dots + D_{\Delta t, 2}(\mathbf{u}_2^{j-1}, p_2^{j-1}, w_2) + D_{\Delta t, f}(\mathbf{u}_1^{j-1}, \mathbf{u}_2^{j-1}, \mathbf{U}^{j-1}, P^{j-1}, w_f).
\end{aligned}$$

3.2 FEniCS

In what follows we describe the implementation of the discrete problem (2.29). We chose *Finite element (FE) programming* in *Python* based on the software library **FEniCS** [2], for our work. *FEniCS* is an open-source computing platform for solving PDE, which turns mathematical models to effective *FE* code. The beginnings of the *FEniCS* project are dated to 2013 when the research cooperation between *University of Chicago* and *University of Chalmers* started.

The software library *FEniCS* consists of a few core components. One of them is *DOLFIN*. It is a *C++/Python* library offering the main user interface and providing a major part of *FEniCS* functionality, like definition of data structures and algorithms. The solving environment for PDEs is also implemented in this library.

The generation of finite elements (e.g. Lagrange element, Raviart-Thomas element) is provided by *FIAT* software, which is also in the *FEniCS* structure.

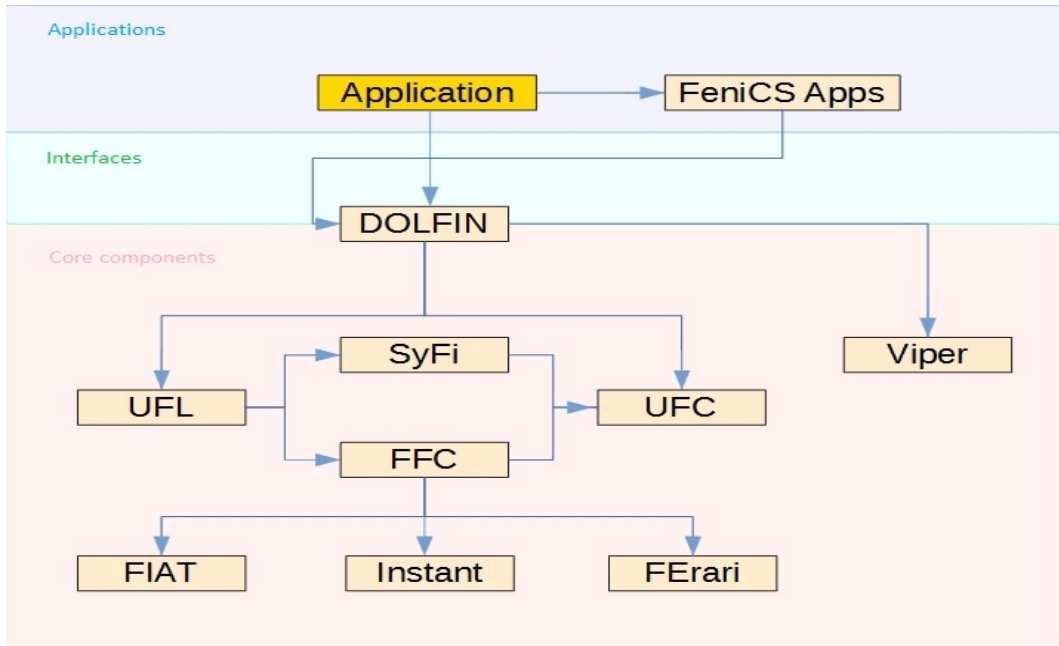


Figure 3.2: *The components of FEniCS.*

FEniCS programs can be coded in *C++/C* and also in *Python*. The module *Instant* is offering the possibility of using *C++/C* typing in *Python* environment. And it makes *FEniCS* more flexible.

Very useful modules are *UFC*, a unified framework for *FE* assembly, and *UFL*. *UFL* enables us to declare the *FE* discretization of the weak form. We also can choose the *FE* space and define an expression for the weak form in mathematical notation. *AsCot*, *Dorsal*, *Syfi*, *Viper* are remaining modules used in *FEniCS*. The main benefit of solving PDE in *FEniCS* is the *UFL* module, which allows to solve PDE's equations only by using the weak formulation of a problem. There is no need to assemble the algebraic system. It is automatically created from the weak forms.

Currently, we adduce how similar is *FEniCS* typing to mathematical notation. The space \mathbb{V}_h can be implemented as:

```

# Define function spaces
# pressure in domain
FE_p = FiniteElement('DG', triangle, 1)
# pressure in fracture
FE_pf = FiniteElement('CG', triangle, 1)
# displacement in domain

```

```

VE_u = VectorElement('DG', triangle, 1)
#displacement in fracture
VE_uf = VectorElement('CG', triangle, 1)
# solution space
W = FunctionSpace(
    mesh, MixedElement(FE_p, FE_pf, VE_u, VE_uf) )

```

where the string `CG` defines a type of the element, in this case it is the *Lagrange element*. There is also possible use *Discontinuous Galerkin (Lagrange) element* and in these cases the first parameter is not `CG` but `DG`. `FEniCS` is not able to define functions which contain only situate/localized discontinuities. However, the trial functions p , u have to be discontinuous on the fracture boundaries. We solved this problem by using `DG` elements which are manually connected by penalization in the bilinear forms. The second parameter selects the type of simplex e.g. `triangle`. Of course, *FEniCS* supports all simplex element families. The third parameter (e.g. 1) determines the degree of the *FE*.

In mathematical problems, there always has to be clear, where the solution and test functions are defined (in which space). It is the same in *FEniCS*:

```

#unknowns
(p, P, u, U) = TrialFunctions(W)
#test functions
(w, wf, r, rf) = TestFunctions(W)

```

The greatest advantage of using *FEniCS* is the natural defining of variational forms. For example, we can take our E_1 form, in mathematical notation written as:

$$E_1(\mathbf{u}_1, p_1, \mathbf{r}_1, \mathbf{U}) = - \int_{\gamma_1} \mathbf{Q}_1 \cdot \mathbf{r}_1 + \int_{\Omega_1} (\mathbb{C}_1 \varepsilon(\mathbf{u}_1)) \cdot \nabla \mathbf{r}_1 - \alpha \int_{\Omega_1} p_1 \nabla \cdot \mathbf{r}_1.$$

In *FEniCS* it will be implemented as follows:

```

#Elasticity equation for the whole bulk domain Omega_1,2
E_omega = (
    -inner(Q_1, r('+'))*dS(region_frac)-\
    inner(Q_2, r('-'))*dS(region_frac)+\
    inner(CE(u), epsilon(r))*dx-alfa*p*div(r)*dx
)

```

The symbols \mathbf{dx} and \mathbf{dS} represent the integration of expressions over the bulk domains Ω_i and over the fracture domain γ .

Our model is an *initial-boundary-value problem*. We used *Dirichlet* (2.29d, 2.29e) and *Neumann* (2.29f, 2.29g) boundary conditions in our system (2.29). *FEniCS* supports all types of boundary conditions (*Dirichlet*, *Neumann*, *Robin*, *Mixed*), but only for *Dirichlet*, *FEniCS* has a special functionality. The other ones have to be implemented by the user. For example, if we want to define this *Dirichlet* boundary condition:

$$P = 0, \mathbf{U} = \mathbf{0} \quad \text{on} \quad (0, T) \times \Gamma_i,$$

in *FEniCS*, we can do it as:

```
#pressure Dirichlet BC for the bulk boundary Gamma_7
bc_p_b = DirichletBC(
    c_p, Constant(0), bc_regions, 7, 'geometric'
)
#displacement Dirichlet BC for the bulk boundary Gamma_7
bc_c_b = DirichletBC(
    c_u, Constant((0,0)), bc_regions, 7, 'geometric'
)
```

The first parameter `c_p` is an unknown, which value is equal to the second parameter `Constant(0)`. The list of the boundaries can be defined as the third parameter `bc_regions` and the number 7 on the fifth position refers to the particular boundary from the list. On the last position, we determine a type of algorithm to decide whether a point lies on the boundary (e.g. `'geometric'`).

As we mentioned before, the analytical solution of our problem is not known in general. In this work, we defined a variational problem (2.45). If we want to find a numerical solution with help of the *FEniCS* library, the notation of the problem is closely similar.

```
#solution
solve(a == L, sol, bcs,
      solver_parameters={'linear_solver': 'lu'})
```

We will use a built-in function `solve()`. First we have to define a variational formulation of numerical problem (e.g. `a == L`), it is exactly like in the mathemat-

ical notation. The variable `sol` hides a sextuple of solution functions. Obviously, it is possible to extract a specific component of solution sextuple (e.g. pressure: `sol.sub(0)`). The last necessary parameter `bcs` refers to a collection of boundary conditions. These three parameters are compulsory. Next parameters identify a *solver*. We use a *linear LU solver* (`solver_parameters={'linear_solver': 'lu'}`). Sparse *LU* decomposition is used by default to solve linear systems of equations in FEniCS programs. This is a very robust and easy to use method. But for larger problems it can occupy really huge amount of PC memory. Large problems is better to solve by using *iterative solvers*, which can be more efficient in terms of both memory and computational time e.g. *Krylov solver* (`solver_parameters={'linear_solver': 'gmres'}`).

3.3 Simulations

Until now, we have presented only theoretical results of our work. Now, we move on our attention to specific application of our model.

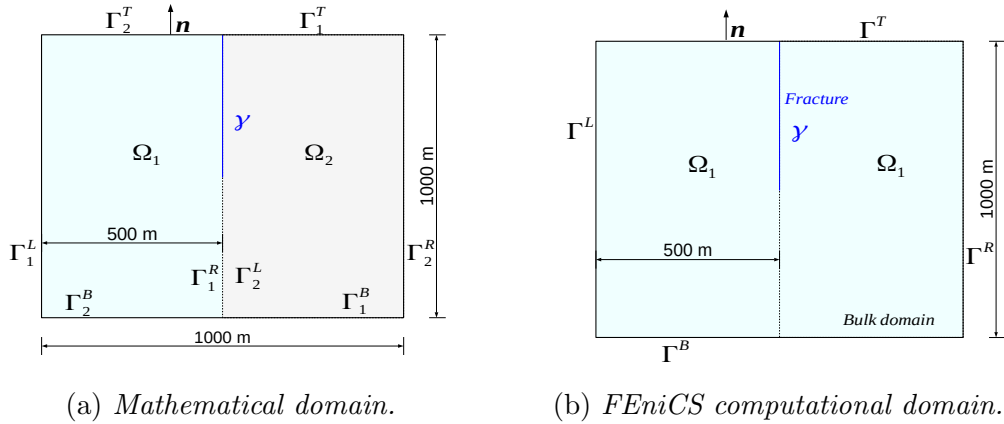


Figure 3.3: *Geometry of computational domain.*

This application has not ambition to simulate real processes in porous medium. We wanted to create a computational domain, which is simple and also can capture full functionality of our model. The computational domain is a 2-dimensional square, see Figure 3.3. In Figure (3.3a), we can see that the computational domain consists of 2 bulk subregions Ω_1 , Ω_2 and a reduced fracture γ . Contrary of the theoretical domain mentioned above (2.1), where the fracture divides the whole domain Ω , here (3.3a) a fracture tip is located in the middle of the square domain. We changed the fracture length for better visualization of our simulation results.

There is another difference to theoretical Ω , simplification the bulk domains Ω_1, Ω_2 . We assume that the fracture is located inside the monolithic rock block. This implies that Ω_1, Ω_2 are made of the same material. Then we can consider only 1 bulk domain (Ω_1), see Figure 3.3b.

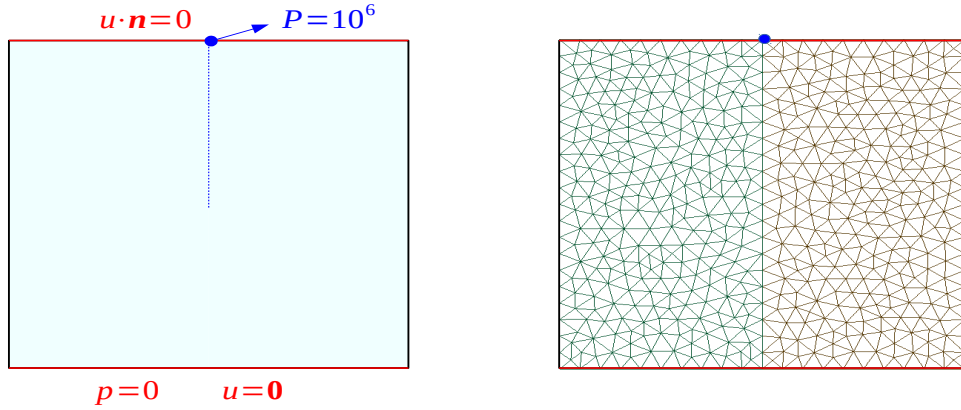


Figure 3.4: (Left): Boundary conditions (Dirichlet), (Right): Meshed domain for Simulation 1.

We computed two simulations. In both of simulations we used the same boundary and initial conditions. On the *top* boundary Γ^T we defined *Dirichlet* boundary condition (BC) for displacement ($\mathbf{u} \cdot \mathbf{n} = 0$), the movement in *normal* direction is not allowed. In the middle of Γ^T , where the fracture starts, the value of fracture pressure was set to $P = 10^6$. This condition simulates impact of high pressure of fracture fluid, which is pumped to the well. On the *right* Γ^R and *left* Γ^L boundary no *BC* was set, explicitly. When *BC* are not set, FEniCS implicitly assumes a zero *Neumann BC* on these boundaries. This setting allows to simulate an expansion of fracture in *tangential* direction. On the *bottom* Γ^B we defined a zero *Dirichlet BC* for the pressure ($p = 0$) and also for the displacement ($\mathbf{u} = \mathbf{0}$), see Figure 3.4(Left).

Simulation 1 and *Simulation 2* differ in meshing. The mesh in *Simulation 1* is quite uniform and consists of 1034 elements, see Figure 3.4(Right). In the *Simulation 2* we created $3 \times$ finer mesh in the surrounding of the fracture start. This mesh contains 1462 elements. All constants and parameters which are needed

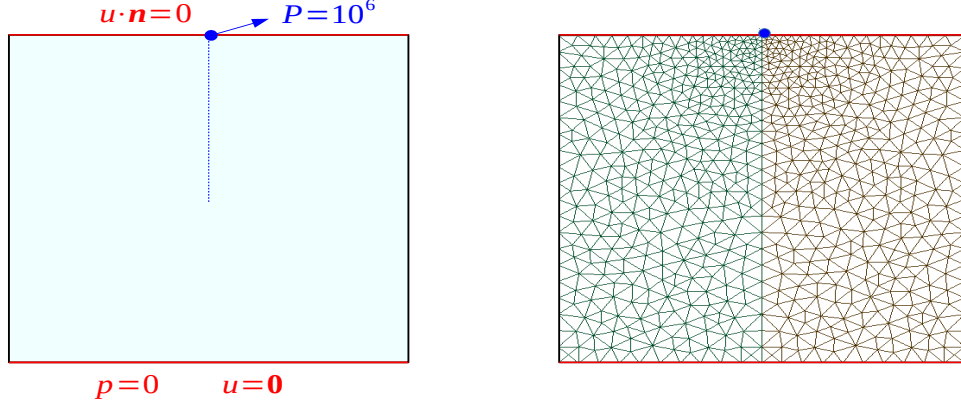


Figure 3.5: (Left): Boundary conditions (Dirichlet), (Right): Meshed domain for Simulation 2.

to set in the simulation are noted in Table 3.1.

MODEL PARAMETERS			
Δt	1000	number of time-step	1000
d	0.1		
S	10^{-5}	S_f	10^{-5}
α	1	α_f	0.4
\mathbb{K}_1	10^{-6}	\mathbb{K}_f	10^{-2}
μ	$1 \cdot 10^{10}$	μ_f	$2 \cdot 10^7$
λ	$2 \cdot 10^{10}$	λ_f	$1 \cdot 10^7$
f	0	F	0
g	$\mathbf{0}$	G	$\mathbf{0}$

Table 3.1: Model parameters (in [SI]).

As we mentioned above, the main function of our simulation is not prediction of the processes in earth crust exactly, so tolerance of little imprecisions in setting of model parameters and constants is allowed. Right setting of physical parameters

would be a task for the geologists. All the constants and parameters used in our simulations (*Simulation 1–S1*, *Simulation 2–S2*) are taken from a range of values usually used in geomechanics and they are listed in Table 3.1. In postprocessing we focus on comparing the pressure and displacement fields of *S1* and *S2*, in times $t = (50\Delta t, 200\Delta t, 300\Delta t, 500\Delta t)$.

In Figures 3.6 and 3.7 we compare pressure fields. For both of simulations *S1* and *S2*, we observe gradual increase of pressure along the fracture. This observation corresponds with the fact, that the bulk domain is solid rock ($\mathbb{K}|_{\Omega} \ll \mathbb{K}_f$, $\mu, \lambda \gg \mu_f, \lambda_f$) and the fracture is a highly permeable and elastic material, which is sequentially filled up by the fracture fluid under high pressure.

In Figures 3.9 and 3.8, we can see the expansion of the fracture in time. Of course, the measure of extension is not in absolute sizes. We enlarged it 1000 times, due to demonstration of results.

The simulations *S1*, *S2* offer almost identical results for pressure and also for the displacement despite of finer mesh in *S2*. It is an important finding for us, because we can avoid using of smaller elements in surroundig of the fracture, by applying reduced fracure instead of conventional domain for the fracture. The discontinuity observed on fracture line (see Figures 3.8a, 3.8c, 3.9a, 3.9c) was occured due to using of DG elements. This problem can be fixed by adjusting of *penalization constant*.

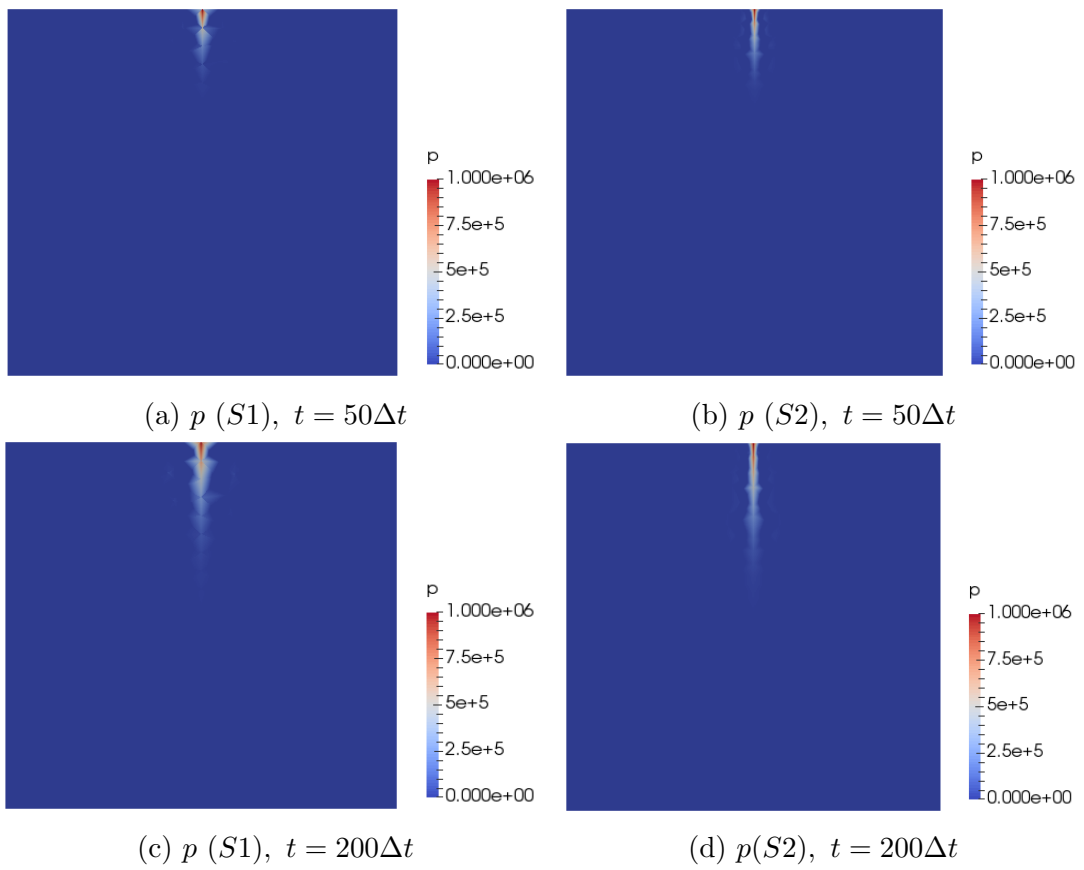


Figure 3.6: Pressure field progress in time $t = 50\Delta t, 200\Delta t$.

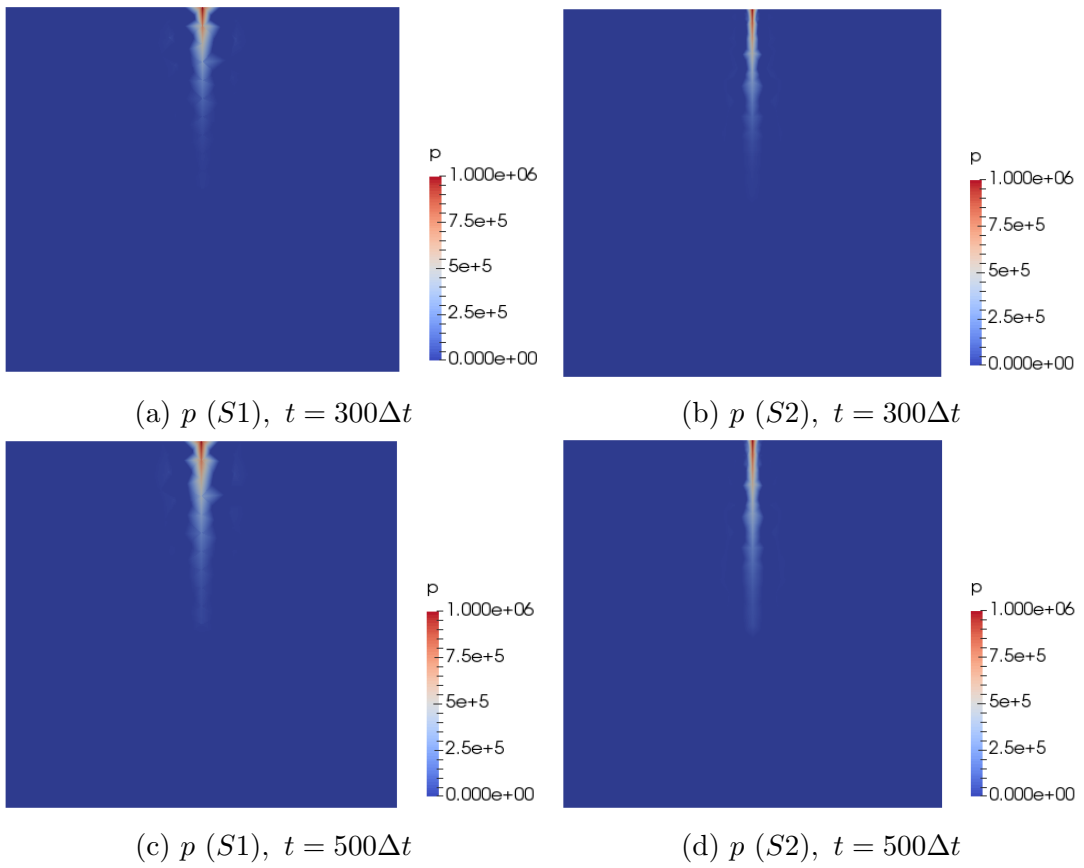


Figure 3.7: Pressure field progress in time $t = 300\Delta t, 500\Delta t$.

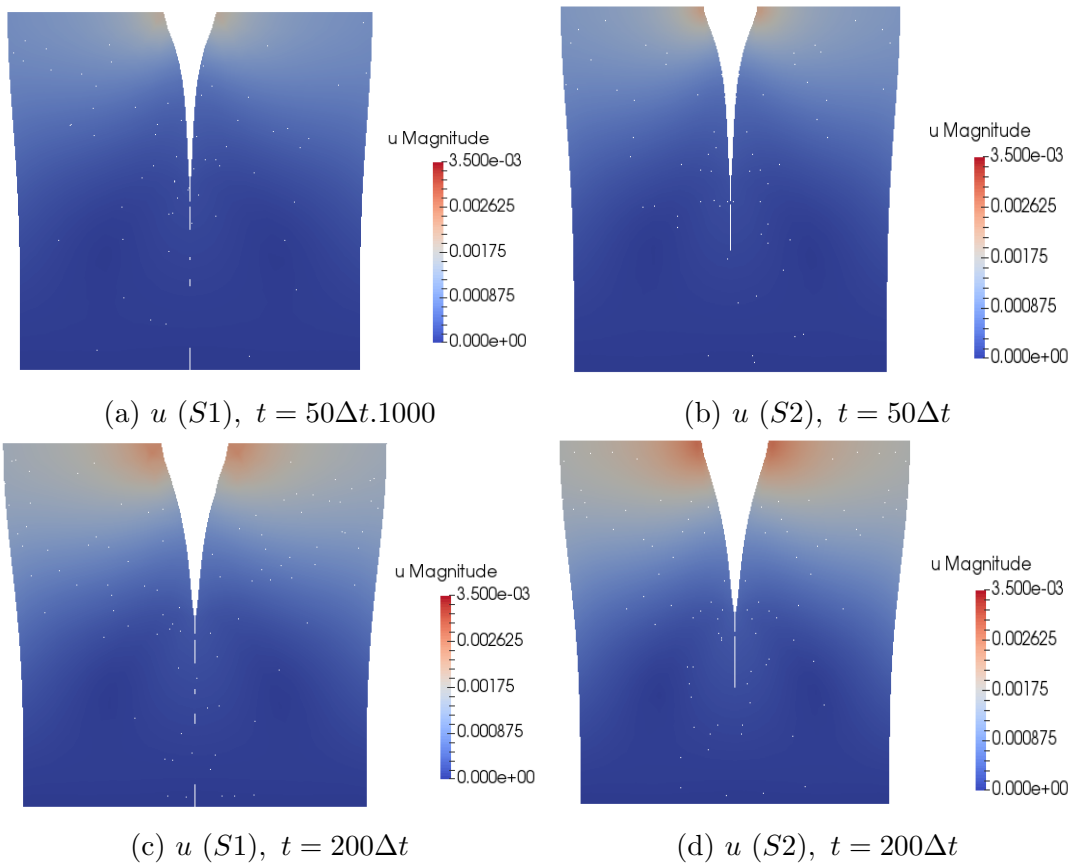


Figure 3.8: *Displacement field progress in time $t = 50\Delta t, 200\Delta t$.*

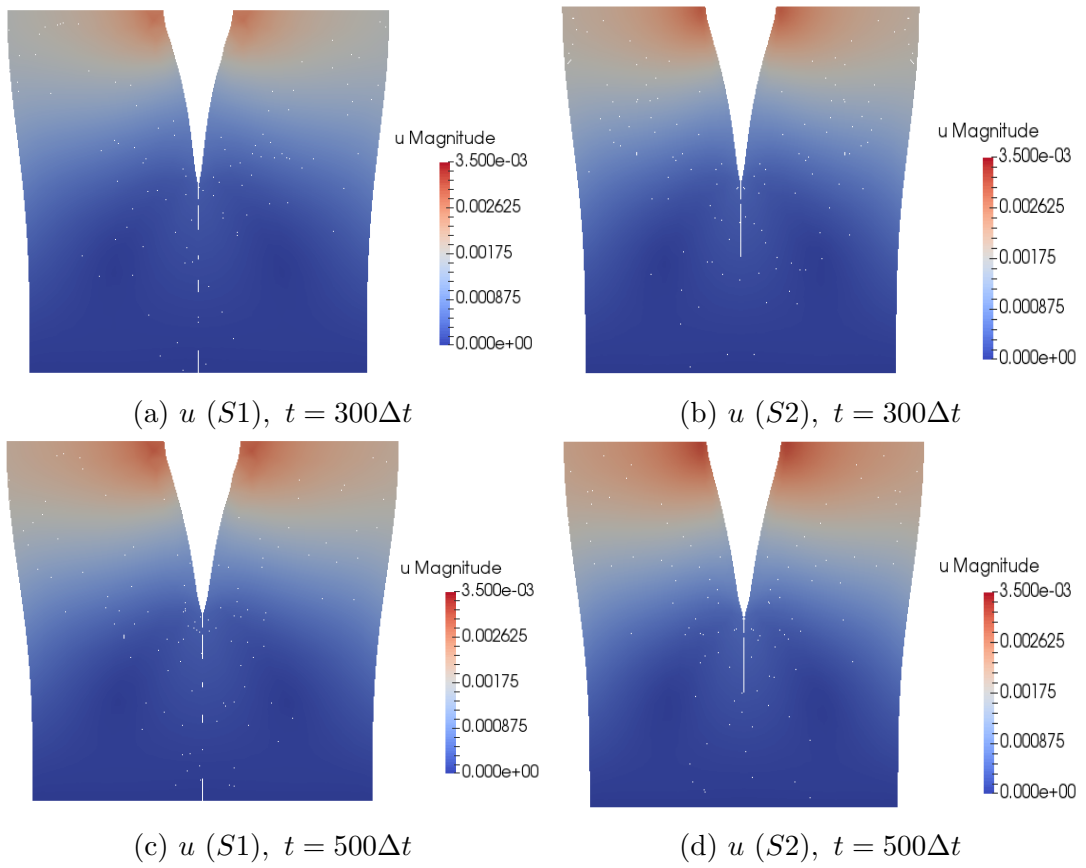


Figure 3.9: *Displacement field progress in time $t = 300\Delta t, 500\Delta t$.*

Summary

Since the work of Biot [3], many publications engaged in research into theory of poroelasticity. Along the progress in computing technology, the dominant theme of poroelastic literature has become the numeric modeling. The poroelasticity is still an open topic and development of new methods steadily continues. This trend is also illustrated by the fact that the publications [13], [11], [12] where we found the main source of inspiration for this work, were published in last two decades.

The most difficult and key part of this work was the derivation of the whole PDE's system for the reduced fracture model (2.29). The principle of reduction of the fracture into lower dimension is not new but the contribution of this work would be, that our model couples reduced elasticity equation and also it is nonstationary in time.

This work also has an ambition to verify function of our model in specific problem through the use of numeric simulations. For the implementation of our model we chose the software library FEniCS. The creation and debugging of FEniCS program was quite difficult for a few reasons. FEniCS supports problems implementation (bilinear and linear forms) in notation highly similar to mathematical formulation, what makes code comprehendible and simple. But for the beginner in FEniCS it is complicated to identify location and cause of bugs in code.

For the purpose of this work, we computed two simple simulations ($S1$, $S2$). On the basis of results (pressure fields in Figures 3.6, 3.7 and displacement vector fields in Figures 3.9, 3.8) offered by these simulations, we could judge that our model works qualitatively properly. It is necessary to mention that mutual ratio of parameters ($d, \mathbb{K}, \mathbb{K}_f, \mu, \mu_f, \lambda, \lambda_f$) has a great impact on solution continuity. In general, the model works more reliably for macroscopic fractures ($d \approx 10^{-2}[m]$). However, if the difference between \mathbb{K}, μ, λ and $\mathbb{K}_f, \mu_f, \lambda_f$ is big enough, the model also offers relatively satisfying results for the fractures of microscopic dimension ($d \leq 10^{-3}[m]$).

Bibliography

- [1] 3 Hot dry rock (HDR) fields. <http://www.open.edu/openlearn/science-maths-technology/science/environmental-science/energy-resources-geothermal-energy/content-section-3>. Accessed: 1999.
- [2] FEniCS Project. <https://fenicsproject.org/>.
- [3] BIOT, M. A. General theory of three-dimensional consolidation. *Journal of applied physics* 12, 2 (1941), 155–164.
- [4] BIOT, M. A. Theory of elasticity and consolidation for a porous anisotropic solid. *Journal of applied physics* 26, 2 (1955), 182–185.
- [5] BIOT, M. A. General solutions of the equations of elasticity and consolidation for a porous material. *Journal of Applied Mechanics* 23, 1 (1956), 91–96.
- [6] BIOT, M. A. Nonlinear and semilinear rheology of porous solids. *Journal of Geophysical Research* 78, 23 (1973), 4924–4937.
- [7] D’ANGELO, C., AND SCOTTI, A. A mixed finite element method for darcy flow in fractured porous media with non-matching grids. *ESAIM: Mathematical Modelling and Numerical Analysis* 46, 2 (2011), 465–489.
- [8] FRIES, T.-P., AND BELYTSCHKO, T. The extended/generalized finite element method: an overview of the method and its applications. *International Journal for Numerical Methods in Engineering* 84, 3 (2010), 253–304.
- [9] GIRAULT, V., KUMAR, K., AND WHEELER, M. F. Convergence of iterative coupling of geomechanics with flow in a fractured poroelastic medium. *International Journal for Numerical Methods in Engineering* 20, 5 (2016), 997–1011.
- [10] H.-D.CHEN, A. *Poroelasticity*. Springer, 2016. ISBN:978-3-319-25200-1.

- [11] HANOWSKI, K. K., AND SANDER, O. Simulation of deformation and flow in fractured, poroelastic materials. *Preprint, arXiv:1606.05765* (August 15, 2016), 1–36.
- [12] LIU, R. *Discontinuous Galerkin Finite Element Solution for Poromechanics*. PhD thesis, December 2004.
- [13] MARTIN, V., JAFFRÉ, J., AND ROBERTS, J. E. Modeling fractures and barriers as interfaces for flow in porous media. *SIAM Journal on Scientific Computing* 26, 5 (2005), 1667–1691.
- [14] MESCHKE, G., AND LEONHART, D. A generalized finite element method for hydro-mechanically coupled analysis of hydraulic fracturing problems using space-time variant enrichment functions. *Computer Methods in Applied Mechanics and Engineering* 290 (2015), 438–465.
- [15] MOËS, N., DOLBOW, J., AND BELYTSCHKO, T. A finite element method for crack growth without remeshing. *International journal for numerical methods in engineering* 46, 1 (1999), 131–150.
- [16] TERZAGHI, K. v. The shearing resistance of saturated soils and the angle between the planes of shear. In *First international conference on soil Mechanics, 1936* (1936), vol. 1, pp. 54–59.
- [17] VERRUIJT, A. Elastic storage of aquifers. *Flow through porous media* (1969), 331–376.

Appendix

Contents of CD

CD contains these files:

- Python (FEniCS) scripts:
 - `dg.py`: special functions for saving solution,
 - `embedded_mesh.py`: functions for fracture mesh,
 - `fracture_model_WF.py`: parameters settings,
 - `problem_well.py`: model implementation, main functionality.
- Description of files for mesh and geometry:
 - `well.geo`: geometry and region description,
 - `well.xml`: mesh in FEniCS format,
 - `well_facet_region.xml`: description of boundaries,
 - `well_physical_region.xml`: description of bulk subdomains,
 - `well.msh`: mesh in GMSH format.

Simulation **run command**:

```
python fractured_model_WF.py problem_well.py
```